AN INVESTIGATION OF STARTING TECHNIQUES FOR INWARD TURNING INLETS AT FLIGHT SPEEDS BELOW THE ON-DESIGN MACH NUMBER

THESIS

John D. Mack, Ensign, USNR

AFIT/GAE/ENY/05-J07

DEPARTMENT OF THE AIR FORCE
AIR UNIVERSITY

AIR FORCE INSTITUTE OF TECHNOLOGY

Wright-Patterson Air Force Base, Ohio

The views expressed in this thesis are those of the author and do not reflect the official policy or position of the United States Air Force, Department of Defense, or the U.S. Government.

AFIT/GAE/ENY/05-J07

AN INVESTIGATION OF STARTING TECHNIQUES FOR INWARD TURNING INLETS AT FLIGHT SPEEDS BELOW THE ON-DESIGN MACH NUMBER

THESIS

Presented to the Faculty

Department of Aeronautics and Astronautics

Graduate School of Engineering and Management

Air Force Institute of Technology

Air University

Air Education and Training Command

In Partial Fulfillment of the Requirements for the

Degree of Master of Science in Aeronautical Engineering

John D. Mack, BS

Ensign, USNR

June 2005

AFIT/GAE/ENY/05-J07

AN INVESTIGATION OF STARTING TECHNIQUES FOR INWARD TURNING INLETS AT FLIGHT SPEEDS BELOW THE ON-DESIGN MACH NUMBER

John D. Mack, BS
Ensign, USNR

Approved:

_____/signed/_____ _____
Dr. Milton E. Franke (Chairman) Date

_____/signed/_____ _____
Dr. Mark F. Reeder (Member) Date

_____/signed/_____ _____
Raymond C. Maple, LtCol, USAF (Member) Date

Abstract

The purpose of this study was to create and investigate starting techniques aimed at allowing complex, three dimensional inward turning inlets to start by swallowing the shock wave associated with un-started inlets. The designed techniques were rooted in supersonic diffuser theory and the Kantrowitz limit, and the techniques attempted to alleviate the over contraction that occurs in inward turning inlets at flight speeds below the on-design Mach number. Five cases, three geometries at two flow conditions, and the base non-modified inlet at the two different flow conditions were generated and all were numerically simulated using a commercially produced numerical solver, CFD++. The simulations were computed using the inviscid Navier-Stokes/Euler equations in a steady state analysis to generate the shock wave, followed by a transient analysis to allow the shock to move in time. The results of the investigation show that all five cases proved to be sub-optimal as none were able to successfully swallow the shock during the transient simulation. However, the results from this analysis indicate that the slit case, designs that extended the initial spill areas of the inlet, appear to hold the most potential in the creation of a successful starting technique. The slit case holds the most potential because the slit Mach 2.7 case was just as effective as the slot Mach 2.7 case, yet the slit area was half the size as the designed slots. Future research should attempt to characterize the effects of slits at different Mach numbers and at various complexities of inlet and slit geometry.

Acknowledgments

I would like to express my sincere appreciation to my faculty advisor, Dr. Milton Franke, for his guidance and support throughout the course of this thesis effort. I would also like to thank my sponsors; Glenn Liston, Mark Hagenmaier, and Lance Jacobsen, from the Air Force Research Laboratory Propulsion Directorate, for both the support and encouragement provided to me in this endeavor.

John D. Mack

Table of Contents

Page

Page

Page

List of Figures

Page

Page

List of Tables

Page

Nomenclature

Symbol	Description
A	...……Area, or area of wind tunnel test section
A*	...……Choked area
A_{bleed}	...……Area after bleed modifications
AFRL	...……..Air Force Research Laboratory
AMRAAM	...…….Advanced Medium Range Air to Air Missile
A_{req}	….Area required to allow a supersonic diffuser to start
A_{throat}	……..Area at the diffuser throat
At1	……...Area at the wind tunnel inlet throat
At2	……..Area at the wind tunnel diffuser throat
BC	……..Boundary Condition
BVRAAM	...……Beyond Visual Range Air to Air Missile
β	……...Coefficient of Thermal Expansion
CAD	……..Computer Aided Drafting
CFD	…….Computational Fluid Dynamics
c_p	…….Isobaric Specific Heat Capacity
CR	……...Contraction Ratio
δ_t	……...Time Step
F_i	……Body force in Index Notation
g_i	……...Gravitational Force in Index Notation
L	……Length
LO	…….Low-observable
M_i	…….Mach number at location i
λ	……Eigenvalue
Λ	……Thermal Conductivity
p_{01}	……..Stagnation pressure in front of a shock wave
p_{02}	…….Stagnation pressure behind a shock wave
P	……..Pressure
ρ	…….Fluid Density
RFP	……Request For Proposal
t	……..……Time
T	……...Temperature
u_i	……Velocity in Index Notation
U	…….Free Stream Velocity
VFDR	……Variable Flow Ducted Rocket
x_i	…….Cartesian Position in Index Notation

AN INVESTIGATION OF STARTING TECHNIQUES FOR INWARD TURNING INLETS AT FLIGHT SPEEDS BELOW THE ON-DESIGN MACH NUMBER

I. Introduction

Background

The Air Force Research Laboratory (AFRL), in conjunction with the Raytheon, Aerojet and Pyrodyne corporations, has attempted to fulfill an RFP from the Variable Flow Ducted Rocket Flight Vehicle Concepts (VFDR FVC) program. In response to the given guidelines, the group constructed the Mustang II inlet presented in Figure 1; a streamline traced, inward-turning, mixed compression inlet.

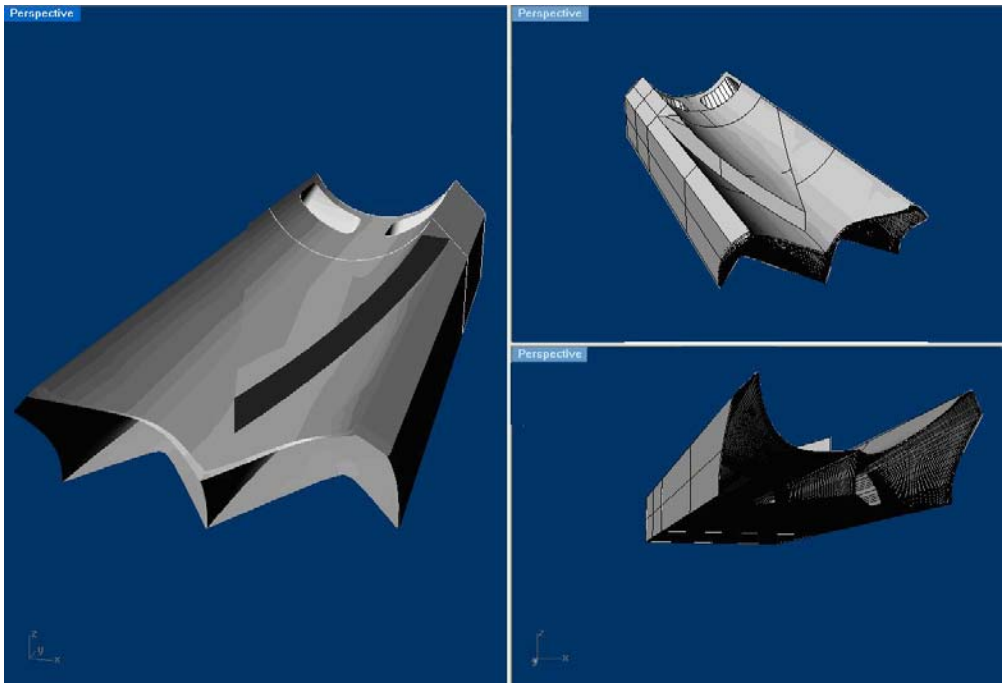

Figure 1. Mustang II Inlet, Rhinoceros CAD Images

Initial CFD analysis of the inlet, by AFRL, at cruise conditions revealed that the inlet held promise in meeting the given RFP. Also, it performed better than the previously designed external compression inlet (9). The CFD analysis, however, was performed on a pre-started inlet operating at cruise conditions. Initial experimental testing, on the other hand, showed that the inlet failed to start under any Mach number and back pressure combination. This initial failure, a common problem for every inlet that relies upon internal compression (or mixed compression inlets that have the majority of the compression done internally), was handled with the current method known to date; bleed holes were drilled at the throat and slightly upstream of the throat and can be seen in Figure 2. The bleed holes were angled toward the free stream and were drilled around the inlet perimeter at both locations.

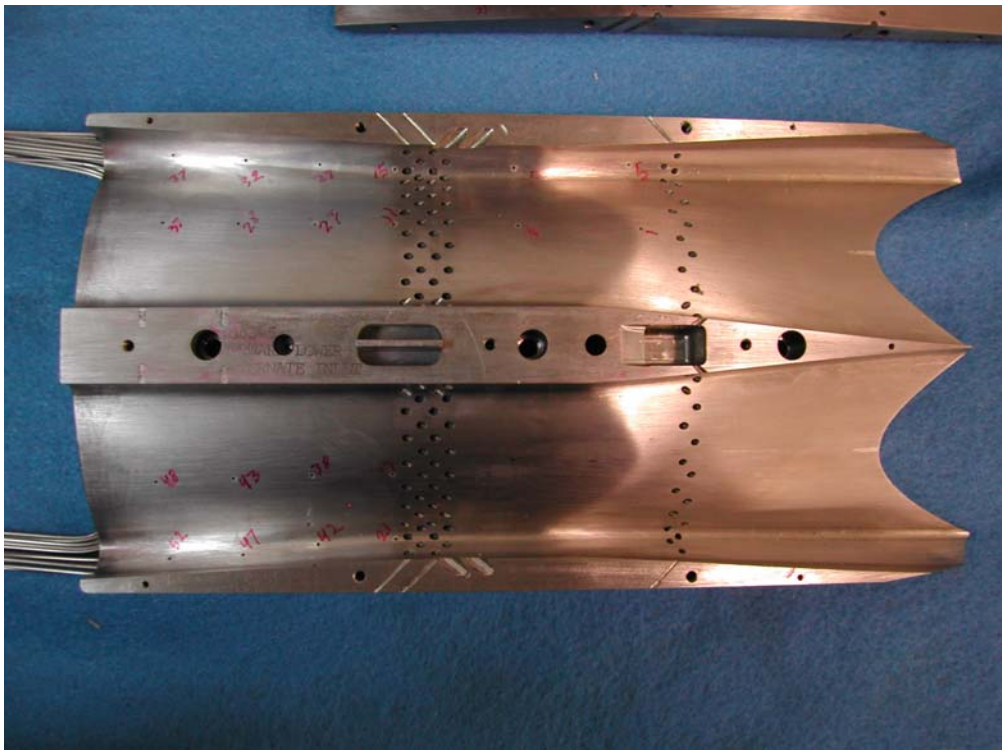

Figure 2. Top Half of the Mustang II Inlet Test Section with Bleed Holes. Flow Direction is Right to Left (9)

Unfortunately, this method failed to rectify the starting problem for the Mustang II inlet (9).

AFRL is now in search of starting techniques to assist the Mustang II inlet project. Overall, a generic, simple, and effective starting technique is needed to provide a baseline start-able inlet for any streamline traced, inward-turning inlet (9).

Variable Flow Ducted Rocket Missiles

In the late 1990s, the European Union began looking for a new medium range air-to-air missile to outfit their new Euro-fighter. While many thought they would simply use the American made AMRAAM missile, the European Union decided, in 1995, to fund the BVRAAM project instead (5). The new project called for longer ranges, linear velocity profiles and better guidance systems (5). Traditional missiles, using existing solid rocket technology, could not accomplish the requirements of the European Union's proposal; therefore, in order to accomplish the design goals, the competing companies turned to VFDR Missiles. In 2000, the European Union awarded their BVRAAM contract to a European contractor and the Meteor Missile, Figure 3, has hence been in development (5).

Figure 3. The European Funded Meteor VFDR Missile (5)

VFDR missiles utilize a hybrid propulsion design; a solid rocket initially accelerates the missile until a designed point where a variable flow ramjet engine can ignite and sustain flight. The design of such missiles is a complex project based on a myriad of options. Internal component layout is complicated as a second source of fuel and ignition systems must be included. Inlets need to not only be constructed on the outer surface in order to capture air for the ramjet inlet, but must also be well designed to minimize drag when the initial solid rocket is accelerating the rocket. Additional computer resources must be created to monitor and adjust the fuel usage of the ramjet engine. New flight control logic, similar to typical fighter aircraft maneuvering, will also be needed as the missile can no longer utilize a skid-to-turn approach because a constant supply of air is needed to reduce the chance of engine flameout.

The magnitude and complexity of these issues is only increased as the Air Force, Aerojet, and Raytheon (one of the BVRAAM competitors) are now trying to change their design to fit the needs of the United States military; namely the new F/A-22 Raptor (9). Reasons for the increased complexity are found in the unique design characteristic of the F/A-22; a low observable (LO), high speed super cruise fighter aircraft with internal weapon carryout. As can be seen in Figure 3, the external inlet design of the meteor missile is a large bulky rectangular design that affects the placement of the aft control fins. Similarly, the baseline VFDR missile follows the same design mentality (9). These large rectangular inlets, plus the displacement of the control fins cause the overall wingspan of the missile to increase from 12.5 inches (19) to more than 20 inches (9). This increase then limits the missiles usefulness as the internal weapons bay of the F/A-22 can

not accommodate these weapons in their current configuration. The F/A-22 can accommodate six standard compact AMRAAM missiles, but would only be able to carry, at most, four VFDR missiles (9). The guidelines given by the VFDR FVC specifically call for an inlet design that would not increase the frontal area of the VFDR missile and hence make it an acceptable replacement for the current compact AMRAAM Missile.

Inlet Design

Traditional inlet design can be separated into three areas; subsonic, supersonic, and hypersonic. Subsonic inlets, the most commonly designed, are generally fairly simplistic design that helps condition the air entering the inlet such that it reaches the compressor face at a suitable Mach number. Recent designs have included beneficial features such as blow-in doors to assist on take-off, or inclined surfaces to assist flight at cruise, but their overall designs have been relatively similar since subsonic cases do not have to deal with shock waves (10).

Supersonic inlets must deal with both subsonic and supersonic flight. This increase in flight envelope greatly complicates inlet design and makes the design a mix of art and tradeoff as one must decide how to proceed. When supersonic flight was first accomplished and became the norm for military aircraft, procedures were created to help design supersonic inlets. Overall, these procedures attempted to simplify the process by making either axi-symmetric or 1-D assumptions in order to simplify the governing equations (15). The equations were still complicated, but computers of the age or hand calculations could accomplish the job. Aircraft today still show the simplifying logic of

these designs as the F-14, F-15, F-18 and even the SR-71 have inlets that rely upon either rectangular external or mixed compression, or axi-symmetric mixed compression inlets.

Recently, the extraordinary increase in computational power has allowed modifications to inlet design, especially as LO technology has been incorporated into such designs as the F/A-22, F-117, and the improved F-18 super hornet. This increase in computational power has also allowed the inlet design community to explore full 3-D inlets. Hypersonic aircraft and more specifically ramjet and scramjet engines have also been a driving factor in the design of highly complicated inlets. In order to accomplish the goals of hypersonic aircraft, most believe that the inlet design will have to be a major design component that will drive the overall shape of the aircraft itself (3,11).

As hypersonic research has continued, streamline traced inlets have become the design of choice. Based on Busemann inlets, streamline traced inlets have a pressure recovery potential near 100%, while external compression inlets are limited by a Mach number dependent pressure recovery potential (8). The design of such inlets is also very useful in the fact that the inlet can be designed to fit nearly any geometry. However, these inlets are hampered by starting problems and often require detailed computer programs in order to create such geometries.

Problem Statement

The problem addressed in this thesis is rooted in all streamline-traced inlet design; the starting problem. While most research to date has been based in streamline tracing design and optimization, significant research is only now being done to specifically address the starting problem; the generation of a shock wave standing outside the inlet

due to over-contraction, an unsustainable pressure increase, through the inlet at the given flight condition. While the problem itself is well known, it was addressed in the early 1940s by A. Kantrowitz (7), very little has been done to create design answers. The most widely used answer to the starting problem is a variable geometry inlet. The inlet is designed to open wide in order to swallow a shock, and is then closed to increase the pressure recovery. While this technique is very successful, it does not help those designs, such as medium range air-to-air missiles, where bulky moving parts add weight and take up space. Simplistic modifications to the inlet are needed in order to help such streamline traced inlet designs; inlet modifications similar to bleed holes that have been successfully used to bleed boundary layers in inlets. This thesis will document the investigation of starting techniques using augmented bleed for pressure relief in streamline traced inlets.

Research Focus

This thesis will focus on the creation and investigation of starting techniques for inward turning streamline traced inlets. Specifically, two techniques will be studied and the techniques will be based in supersonic diffuser theory and the Kantrowitz limit (7). Each technique will specify the location and size of the area to be removed from the inlet. These open areas will alleviate the internal compression and if the assumptions used in the techniques are valid, allow the inlet to swallow the starting shock. Otherwise, the results will lead to modifications of the current designs or reveal insight into other possible techniques.

Methodology

The design of the starting techniques presented is rooted in supersonic diffuser theory and the Kantrowitz limit (2,7). Supersonic diffuser theory gives the simplification of quasi-one dimensional flow and the starting requirement for a supersonic wind tunnel, and the Kantrowitz limit yields the maximum contraction ratio for an inlet at a specified flight Mach number. Both of these principals are widely known and their usefulness has been demonstrated. These principals, along with results from previous bleed hole design research (17), were used to create two unique design methods. Two specific flight conditions for the VFDR missile were chosen and the design methods were applied at each condition.

The resulting designs were modeled using the Rhinoceros NURBS modeling program. These models were then transferred to Gridgen, a commercial meshing program. CFD++, a commercial computational fluid dynamics package, was then utilized to simulate the starting designs while at their specified flight condition. Finally, Tecplot, a commercial data analysis and visualization program, was used to post process the data into easily viewable figures.

The analysis was broken into two stages; first, the design was run in an inviscid steady state model in order to establish the standing shock that will be present when the inlet attempts to start after the missile boost phase. Second, a transient analysis would be run, using the result of the steady state analysis as the initial condition, in order to see how the inlet modifications allow the shock to move in time down the inlet.

Performance Measure

The performance measure will be the ability of the inlet to pass a shock wave. This measure will be accomplished by visualizing the pressure and Mach contours inside the inlet during the numerical simulation. The shock wave will appear as a large discontinuity, or abrupt change in color, in the computational plane, and a successful design will allow the discontinuity to move down the inlet during the transient analysis.

Report Overview

This thesis report will be broken into six chapters: introduction, relevant research, analytical design, numerical simulation, results and discussion, and conclusions and recommendations. The introduction, presented above, covers a background of the problem at hand along with a history of variable flow ducted rockets and inlet design. A precise problem statement along with a general encompassing methodology and performance measure are then described.

The second chapter will present a review of relevant research.

The third chapter will describe the methodology of the starting techniques. A review of the governing equations and assumptions will be stated. The starting techniques will be explained from theory and applied to given cases derived from the missile flight profile. The computer programs used during this part of the analysis will also be described and their use detailed.

The fourth chapter will cover the numerical simulation performed on the starting techniques. The programs used in the analysis will be described, and all relevant information concerning how the designed inlets will be imported to the computational

plain, run through their specific flight case, and exported to the analysis software so that the CFD results can be visualized and understood will be discussed.

The fifth chapter will detail the results of the analyzed cases and offer discussion upon the findings. At this stage, one of the design techniques will be offered as the design choice based upon the ability of the modification to start the inlet and have the best performance, or the modification that appears to have the best potential to successfully start the inlet.

The sixth chapter will concern the conclusions that can be ascertained by the given results. Closing thoughts and potential future work will be presented as well.

II. Relevant Research

Busemann Inlets

The idea of using Busemann inlets, an axi-symmetric internal flow consisting of an isentropic compression followed by a free-standing conical shock (11), for hypersonic speeds is not new. Research as early as 1966 proposed the use of such inlets, however much of the initial research was concerned with the design and theoretical performance of the inlets. Molder and Szpiro (11) accomplished such research in 1966. Their paper, "Busemann Inlet for Hypersonic Speeds," gives the general design equations for Busemann inlet design, namely the Taylor-Maccoll equation for axi-symmetric flow, and also gives a generic description of the inlet's positive and negative attributes. Positives include the high pressure recovery, simplistic design, and easily determined performance. Negative attributes were physical design limitations (necessity for very long thin inlets that may be structurally impossible to design), self-starting difficulties, and possibly large boundary layer losses due to the inlet length.

Molder continued his research, and along with D. M. Van Wie (21), produced another work; "Applications of Busemann Inlet Designs for Flight at Hypersonic Speeds." This work gives the design equations for Busemann inlets and includes design examples and experiments. An inlet designed for a free stream Mach number of 16 was examined using a space-marching algorithm. This algorithm was used to show the internal flow angle contour plots at three different Mach numbers; 10, 16 and 25. This test was done to show that on the designed Mach number, the Busemann inlet followed

the Taylor-Maccoll equations and established a conically symmetric isentropic compression.

A physical experiment was also conducted on a Canadian National Research Council Busemann inlet that was designed for a free stream Mach number of 8.33. First the inlet flow field was simulated using the PNS SCRINT and its results were compared to the inviscid flow field solution. Second, the boundary layer was modeled using both the PNS and the STAN^ codes. Third, a small model of the inlet was tested at Mach 8.3 in the Joint Ryerson/University of Toronto gun tunnel and at a Mach number of 8 in the Calspan 48 inch shock tunnel. The results of these three experiments yielded favorable agreement. The experiment and the PNS code agreed and closely followed the overall trends predicted by the inviscid predictions.

Streamline Tracing

Streamline tracing has been a rather recent area of research because its methods are highly computer dependent. Billig and Kothari (3) wrote an overview of the streamline tracing methodology and design procedures in their work, “Streamline Tracing: Technique for Designing Hypersonic Vehicles” in 1997. After an initial description of the Busemann inlet design procedure, they generalized the streamline tracing method and introduced the radial deviation parameter. This parameter, which varies from -1 to 1, correlates to the inlet being either outward tuning (a value of -1 and represented by flow moving over a cone), two-dimensional planar (value of 0 and represented by flow between two plates), or maximum inward turning (value of 1 and represented by flow moving through a funnel). Using this parameter, Billig and Kothari

describe the numerical method used in streamline tracing as well as the experimental and theoretical results of an inlet designed using their methodology.

Supersonic Inlet Design

Most of the research expressed above has been for hypersonic design. Supersonic inlet design is more difficult for streamline traced inlets because the starting problem is intensified as the free stream Mach number is lowered (7). Therefore, research was done to examine how this problem can be overcome using today's methods.

Valorani et al. (20) researched air collecting engines in their work "Optimal Supersonic Intake Design for Air Collection Engines (ACE)." ACE provides air for an air collecting plant and a ramjet engine. Their research studied the on- and off-design optimization of such inlets through their full mission and determined that a mixed compression inlet, an inlet that uses both external and internal compression, was the most beneficial. They created a four-phase plan in designing an inlet: select architecture of the inlet, generate the geometry of the inlet, choose to maximize the total pressure recovery or yield a prescribed Mach and flow deviation at the throat, and predict the performance of the geometries under off-design conditions. Overall, their procedure yielded a multi-stage ramp external compression phase followed by an internal compression for the supersonic diffuser. The ramp would produce shocks that met at the cowl lip, and the internal compression area would have shocks from the cowl lip entering the inlet. Most importantly, this inlet has no starting problems due to its use of external compression.

Smart and Texler (16) produced the paper "Mach 4 Performance of Hypersonic Inlet with Rectangular-to-Elliptical Shape Transition." This work is important because

the inlet was designed for a free stream Mach number of 5.7 which can be debated to be either supersonic or hypersonic. Also, the inlet was forced to use bleed holes in order to self-start the inlet. A moving cowl at the rear of the inlet was used to un-start the inlet, generate a standing shock outside of the inlet, and then adjust to the cowl normal position in order to prove the inlet could then re-start after the standing shock wave was established. While the focus of their project was showing the viability of rectangular-to-elliptic inlet design, it is relevant here because it is one of the few works that chronicles the use of bleed holes to assist in streamline traced inlet starting. Their work revealed that bleed between the cowl and inlet throat was more efficient, i.e. allowed the inlet to start with the greatest mass flow rate, then adding holes at the cowl. Also it showed that adding side holes yielded more efficiency per hole than the cowl bleed holes. They did not research the size of holes or their orientation though; all research was done with one eighth inch holes and their orientation, either angled or perpendicular to the flow, was not revealed. Their work confirms that some form of bleed is required to self-start a streamline traced inlet.

Bleed Hole Design

A NASA Contractor Report by Syberg and Hickcox (17) yielded a study of differing bleed hole designs by examining their size, position with respect to each other, and orientation to the flow. Overall their work was to design a bleed system for a Mach 3.5 inlet, but their study of bleed hole design is beneficial for any bleed system whether it be for boundary layer bleed, or pressure relief. With regards to orientation with the flow, their research showed that angling the hole toward the flow increased the hole mass flow

coefficient, the ratio of actual flow to the max theoretical flow at local pressure and temperature. This also showed that as Mach number increased, the effectiveness of the bleed hole decreased. With regards to bleed hole spacing, their work showed that as the ratio of the distance between hole centers and the hole diameter decreased, the bleed flow increased. It is also shown that as Mach number increases, the relative gain in bleed rate is improved by decreasing the distance between the hole centers.

A NACA Research Memorandum by Luidens and Flaherty (8), titled "Use of Shock-Trap Bleed to Improve Pressure Recovery of Fixed and Variable-Capture-Area Internal Contraction Inlets: Mach Number 2.0 to 3.0," showed that shock trap bleed was more beneficial than ram scoop bleed. Ram scoop bleed simply siphons air away from the diffuser; the diffuser would appear as a smaller circle inside the inlet at the throat. Shock-trap bleed puts a shim between the throat and the diffuser so that the diffuser lip is very similar in height to the shim lip. The resulting expansion/shock interaction provided by the shim and relative equal height provides a bleed system that is more efficient than scoop bleed alone. Their report yields an increase in pressure recovery from 0.76 with ram scoop bleed to 0.85 for the shock-trap bleed system at Mach number 2.94.

Modern Research

Research has been initiated in the field of starting techniques for Busemann inlets. An AIAA paper, "Numerical Analysis of Streamline-Traced Hypersonic Inlets," by Tam et al. (18) summarized a computational study of a method to place bleed slots on streamline traced hypersonic inlets. These slots were used to help the inlet start at lower than designed Mach numbers. Their method was centered on the contraction ratio; the

maximum area contraction that still allows a shock wave to be swallowed. Their method calculated the contraction ratio with the free stream Mach number, placed a slot at the downstream position corresponding to the contracted area and then assumed that enough relief was available to allow the shock to swallow. A new Mach number is calculated at this new area and its corresponding contraction ratio. This method is then repeated, placing slots at each contraction ratio, until the inlet throat is reached. Their numerical simulations revealed that the bleed slots were successful and allowed the inlet to start at speeds well under the on-design Mach number. Their research used a lengthy iterative process in order to find the area of each bleed slot. They specify that future research is needed in the sizing of such slots.

III. Analytic Design Process

Chapter Overview

The starting techniques are rooted in two areas of theory; supersonic diffuser theory and the Kantrowitz limit. Both of these theories are well documented and their effects have been repeated in experiments (2,7). These theories will be reviewed in the following section and the incorporation of the theories into the design starting techniques will be stated. The design methods will then be applied to the Mustang II inlet at two specific flight conditions. These two conditions and details of the design modifications will then be detailed.

Supersonic Diffuser Theory

Supersonic diffusers have a wide range of uses, but the one important use in this study is the diffuser of a supersonic wind tunnel. Just like an inlet, a wind tunnel diffuser must slow the flow while using a shock to increase pressure to exit conditions. One of the major simplifications in wind tunnel design is quasi-one dimensional flow (2). This assumption allows one to ignore the effects of velocity in the non-flow direction and assume that as the flow is contracted it only affects the flow in the streamwise direction. The application of quasi-one dimensional flow to a complex three dimensional inlet design is very similar to a supersonic wind tunnel diffuser and would simplify the problem and allow for a design process that concerned itself only with the stream wise velocity.

The Mustang II inlet geometry was designed by Pyrodyne and Aerojet via AFRL/PRA (9). The geometry used in this thesis was modeled in the Rhinoceros

modeling program. Rhinoceros is a NURBS modeling program made for the windows operating system. Specifically made for computer-aided design, the program can output files for computed-aided machining or for other CAD programs for ease of workplace use (13). Rhinoceros also has features that allows for the geometric and structural analysis of generated designs (13).

Using the provided Rhinoceros file, the quasi-one dimensional assumption could be applied to the Mustang II inlet. First, the inlet was cut into 150 slices that could be enclosed using the 'cap' command. The Rhinoceros program then calculated volume, and with knowledge of the height of each slice, the area could be determined. 150 slices was determined to be small enough to avoid large area discontinuities and provide a smooth fit for the area of the inlet as a function of depth into the inlet. The plot of the non-dimensional area as a function of depth is given as Figure 4.

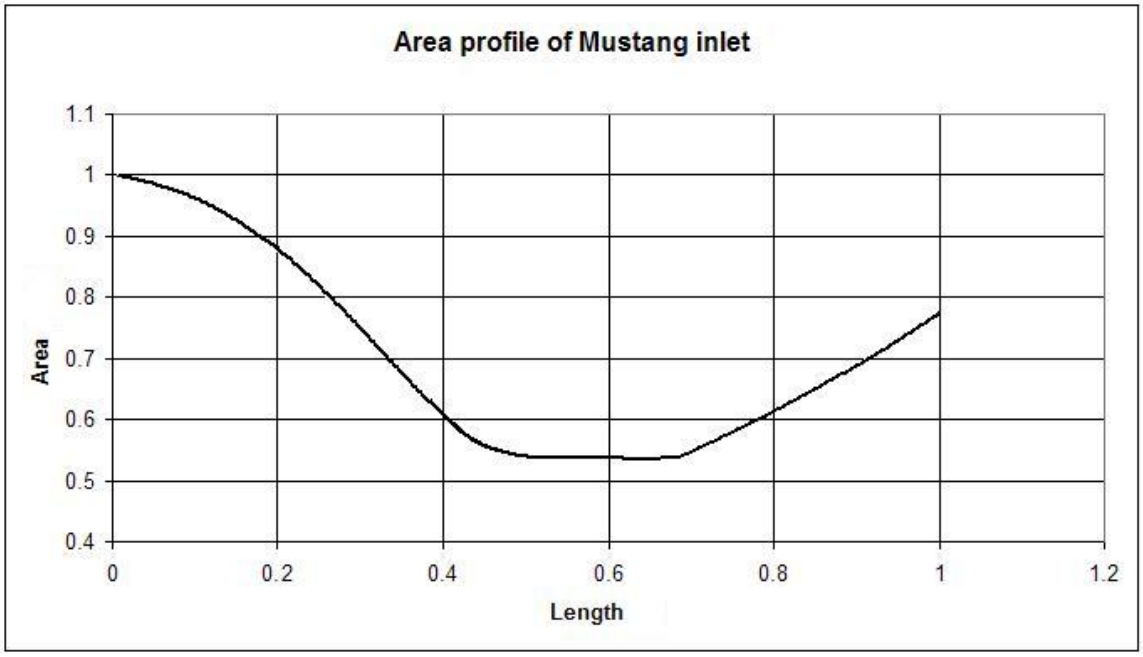

Figure 4: Non-dimensional Area Profile of the Mustang II Inlet

Supersonic diffusers also have a well defined starting requirement. Using the assumptions of choked flow at the throats, adiabatic and isentropic flow, and the equation of state, one arrives at the following relationship between the throat areas,

$$At2/At1 = p_{01}/p_{02} . \quad (1)$$

The derivation of this relationship between the throat areas and the stagnation pressure across a normal shock at the test section Mach number can be found in most compressible flow books, such as reference 2. While an inlet is only the diffuser portion of a supersonic wind tunnel, one can assume that infinitely far away there is a first throat that allows the flow tube that enters the inlet to accelerate to the free stream supersonic Mach number.

Kantrowitz Limit

The Kantrowitz limit was first described in reference 7 in 1945 and an overview of this limit is described henceforth. The limit gives the maximum permissible contraction ratio for a supersonic diffuser. In words, the Kantrowitz limit is defined as the result of multiplying the total head loss across a normal shock by the isentropic area-contraction ratio from a Mach number to the local velocity of sound. Figure 5 is given as reference for the analogy of the Kantrowitz limit to a supersonic diffuser.

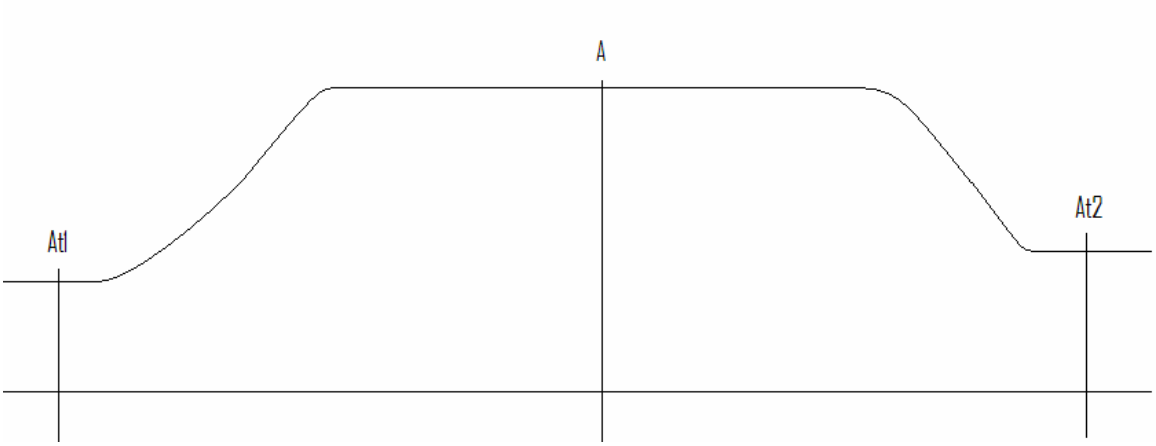

Figure 5: Supersonic Diffuser Example

The isentropic area ratio, or the area Mach number relation (2), gives the ratio between the area of a choked throat and the area of a second throat where the flow is either isentropically accelerated to supersonic speeds or decelerated to subsonic speed,

$$\left(\frac{A}{A^*}\right)=\frac{1}{M}\left[\frac{2}{\gamma+1}\left(1+\frac{\gamma-1}{2}M^2\right)\right]^{\frac{\gamma+1}{2(\gamma-1)}} \tag{2}$$

From Figure 5, this would be the ratio of A to At1, or the area of the tunnel test section area to the first throat. Eq. (1) shows that the total pressure head loss across a normal shock at the test section Mach number was equal to the ratio of the first and second throats. In the following equation, one can see that these understandings imply that the contraction ratio is the maximum ratio of the tunnel area to the second throat area,

$$CR=\left(A/A^*\right)\left(p_{02}/p_{01}\right)=\left(A/At1\right)\left(At1/At2\right)=\left(A/At2\right) \tag{3}$$

Design Methodology

Using the above mentioned theories, two methodologies have been created in order to allow starting in inward-turning inlets: slots and slits. Slots are similar to rows

of bleed holes, but they are much larger in order to relieve more than just the flow boundary layer. Slits are an extension of the spill area already deigned in the inlet due to the streamline tracing technique. Both methods will relieve the internal contraction so that the shock may pass through the inlet throat. In summary, both methodologies rely on the following assumptions,

- The highly three dimensional streamline traced inlet can be modeled as a quasi-one dimensional flow, like a supersonic wind tunnel.
- Velocity changes inside the inlet will be calculated by the isentropic area contraction equation.
- The transient shock will be assumed to stand just outside of the inlet where the internal contraction begins. The steady state shock wave, when the flow is not allowed to flow through the inlet, will stand much farther outside of the inlet.

Slot Design Procedures

The downstream position of the slots is calculated in the same manner as presented by Tam (18). The procedure is repeated here for completeness in describing the design.

1. Calculate the contraction ratio for the given free stream Mach number.
2. Use the contraction ratio to determine the area downstream of the inlet which would allow the inlet to start and use the isentropic area contraction equation to determine the Mach number at this new area. The isentropic area contraction is generically presented as Eq. (4),

$$\frac{A_0}{A_1} = \frac{\frac{1}{M_0}\left[\frac{2}{\gamma+1}\left(1+\frac{\gamma-1}{2}M_0^2\right)\right]^{\frac{\gamma+1}{2(\gamma-1)}}}{\frac{1}{M_1}\left[\frac{2}{\gamma+1}\left(1+\frac{\gamma-1}{2}M_1^2\right)\right]^{\frac{\gamma+1}{2(\gamma-1)}}}, \qquad \text{Eq. (4)}$$

where A_0 and M_0 are the area and Mach number at some position, A in reference to Figure 5 for the first contraction ratio, and A_1 and M_1 are the area and Mach number at the downstream position, some area between A and At2 in Figure 5 (18).

3. Assume that appropriate bleed is accomplished so that the shock wave will move to the smaller area.
4. Calculate a new contraction ratio with the Mach number at this new area and repeat until the contraction ratio yields an area smaller than the inlet throat.

Figure 6 gives a graphical representation to this procedure.

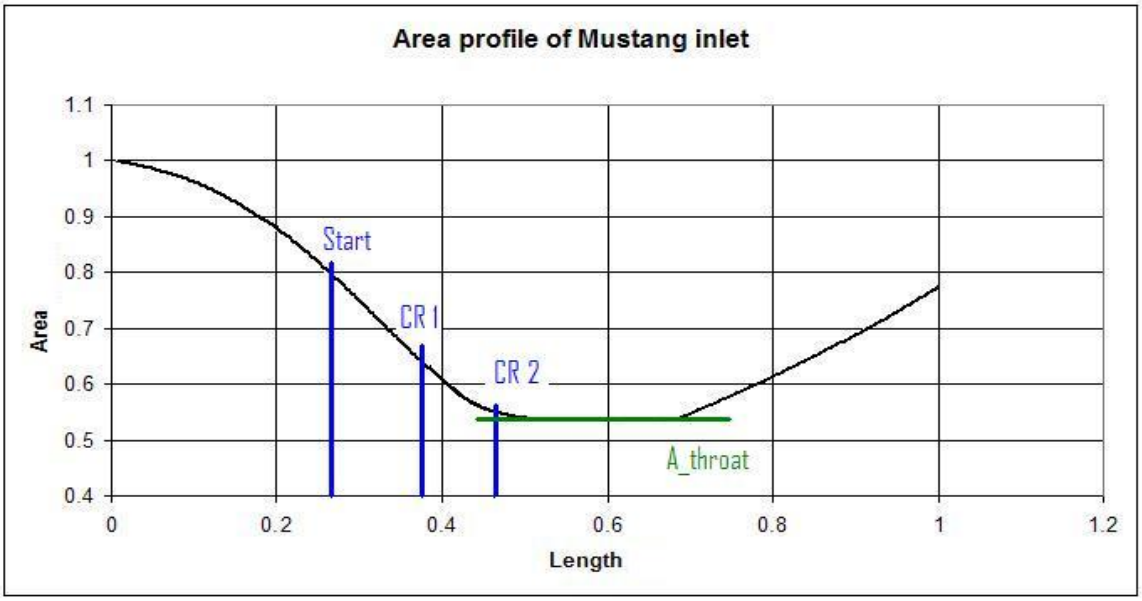

Figure 6: Example of Slot Position Calculation

The area calculation for each slot is calculated by the following procedure.

1. The contraction ratio for each slot gives the location of the area required to start a supersonic diffuser. By subtracting the throat area from this required area one finds the required flow area that needs to be bled.
2. An individual slot is sized by examining the areas required for all the slots. The second, third, etc. slots will assist the first slot in relieving pressure. Therefore, the area for the first slot is the required additional flow area for the first contraction ratio minus the required area for the second contraction ratio.
3. The physical dimension is set by the inlet itself. The bottom of the inlet was chosen as the location for the slot since the bottom is very thin and its geometry is relatively constant as one proceeds into the inlet. Therefore the width of the slot is set by the width of the inlet at that area, and the back end of the slot rests on the location given by the contraction ratio. The length towards the mouth of the inlet is determined by modifying the required area to account for bleed loses.

Figure 7 is a physical interpretation of this procedure.

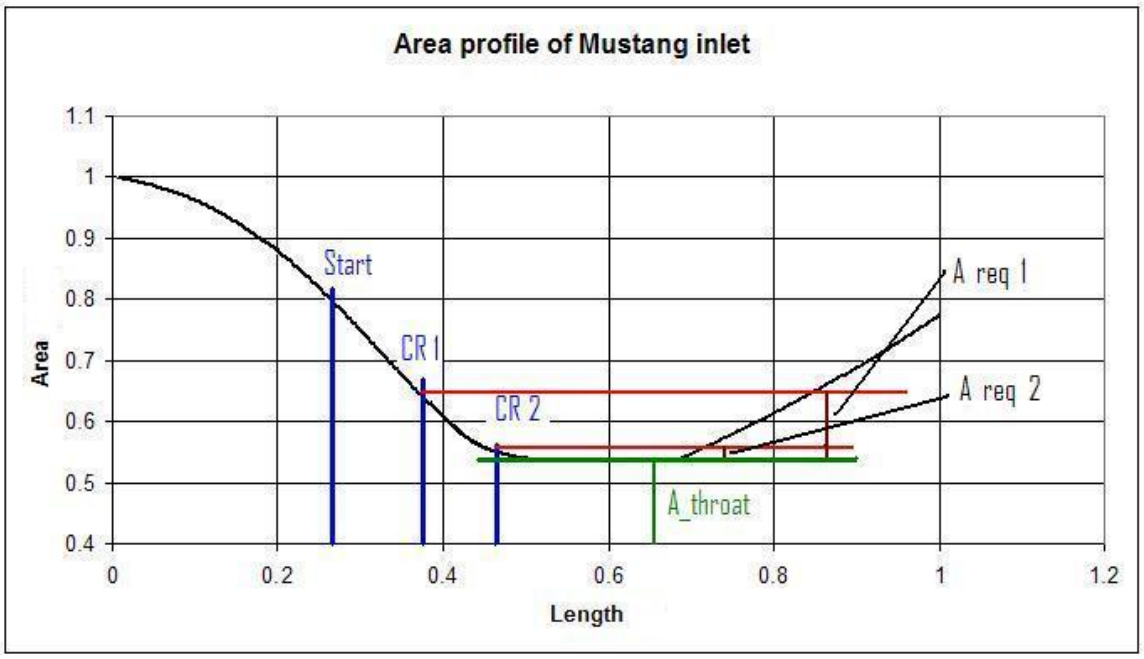

Figure 7: Example of Slot Area Calculation

Bleed Hole Area Losses

The area required for each slot will increase due to losses incurred by changing the flow direction. As stated in the relevant research portion of this thesis, bleed hole research has already been conducted and the important results were stated. From that research it is inferred that slots will provide better bleed flow than bleed holes and that either subsonic flow or choked flow would exist at the slots during inlet starting. The bleed slot angle has an effect upon the bleed flow, but the chosen angle will be based on this effect and ease of manufacturing since the bottom of the Mustang II inlet is thin.

Slit Design Procedures

The slit design is an iterative process and requires an extra assumption. It is assumed that the extension of the spill area will be so large that the shock will pass to the

new start of the internal contraction. With this new assumption, the slit is designed with the following procedure.

1. Guess a Mach number lower than the free stream Mach and calculate the contraction ratio. Use this contraction ratio to find the area upstream of the inlet throat.
2. Find the area corresponding to the condition where the free stream flow is isentropically slowed to the assumed Mach number.
3. Iterate the guessed Mach number until the two areas converge.
4. The area represents the position of the new internal contraction crotch.

Figure 8 is a physical representation of this procedure.

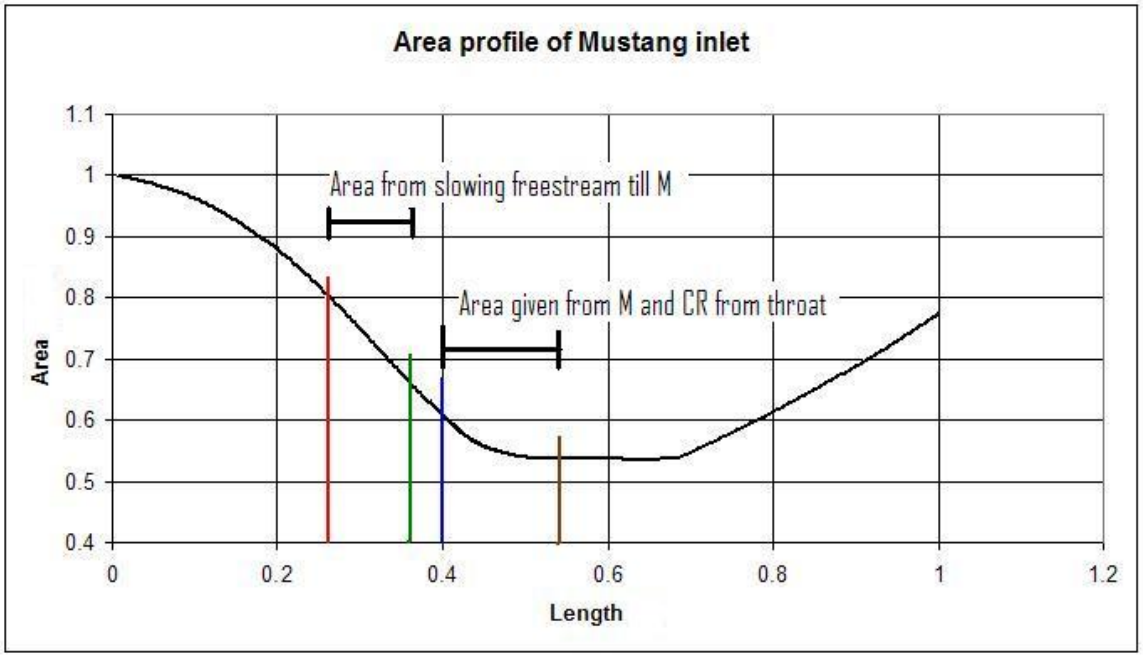

Figure 8: Example of Slit Crotch Location Calculation

This process ensures that if the flow can isentropically slow from the capture area to the contraction area, then the given Mach number at the new crotch, the location of the designed contraction area, will be able to pass a shock through the inlet throat.

The physical dimension of the slit does not have an area requirement like the slot method. However, the area needs to be large enough in order to ensure the validity of the new assumption for the slit case. A reasonable area size is the area that results from subtracting the area of the inlet at the new crotch from the total inlet capture area. This is reasonable because as the free stream Mach number increases, the new crotch will advance towards the mouth of the inlet meaning the area at the crotch will be larger and the difference between this area and the total capture area will decrease. At the same time as the free stream Mach is lowered, the difference in area will increase and the slit area will increase. The angle of the slit is up to the designer, but with the above area and a known length into the inlet, one could calculate an angle to give the triangle area for the slit extension. A triangle area is chosen in this case for ease of modeling.

Modifications to the Mustang II Inlet According to Design Methodology

Two flight conditions were chosen in order to test the above described design methodologies; these conditions are an altitude of 10 km at a Mach number of 2.7, and an altitude of 1 km at a Mach number of 2. The 10 km and Mach number 2.7 condition represent a normal long range missile intercept. The 1 km and Mach number 2 condition represent a severe dogfight case. The designs were applied to these two flight conditions and are given a case numbers in order simplify the description process in the proceeding

sections. Table 1 describes each case specifying the design used, altitude, and Mach number.

Table 1. Case Definitions

Case	Design Method	Altitude	Mach Number
Base 1	Unmodified	10 km	2.7
Base 2	Unmodified	1 km	2
1	Slit	10 km	2.7
2	Slot	10 km	2.7
3	Slit	1 km	2
4	Slot	1 km	2
5	Slot, redesigned	10 km	2.7

Case 5 is a redesigned slot case that was created after initial results from the first four cases were interpreted and the two base cases are the unmodified inlet. They were simulated to provide a reference solution for the conclusion of the steady state simulation.

Slot Designs

All slot cases were designed with the same bleed design. With the assumptions stated, and after reviewing the bleed hole research, it was decided that setting the hole angle at forty degrees was the most beneficial and easy to model even though the bottom of the inlet is thin. Also, the bleed research showed that one could expect the bleed slots to be approximately sixty percent effective, so the required area was increased by at least forty percent. This augmentation was easily handled by adding the angled cuts to the required slot area design. Figure 9 graphically represents the slots designed.

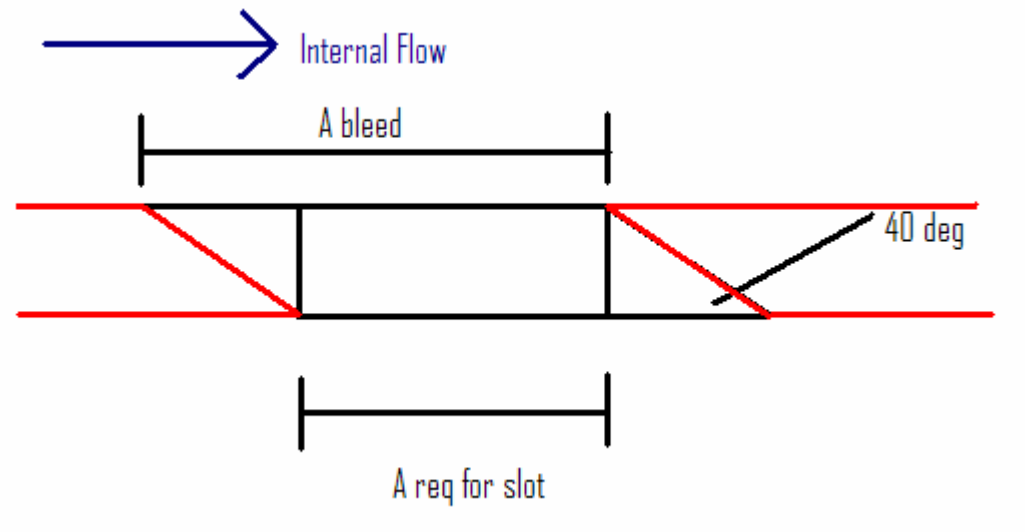

Figure 9: Designed Bleed Slots for Both Cases

Table 2 lists the non-dimensional specifics of the slot designs for each case. The slot location is measured from the front of the inlet.

Table 2. Nondimensional Slot Design Characteristics

	Back of First Slot Location (x/L)	**Back of Second Slot Location (x/L)**	**Area Required (A/A_{max})**	**Area Designed (A/A_{max})**
Case 2	0.4056	NA	0.0971	0.1759
Case 4	0.3500	0.4222	0.1300	0.3539
Case 5	0.4056	NA	0.0971	0.4247

The area designed for Case 5 was large enough to create two slots; one located on the bottom surface like the other cases, and the other located on the right side of the inlet wall. Figures 10 and 11 show the three designs, as generated in Rhinoceros, so that the different cases can be compared visually.

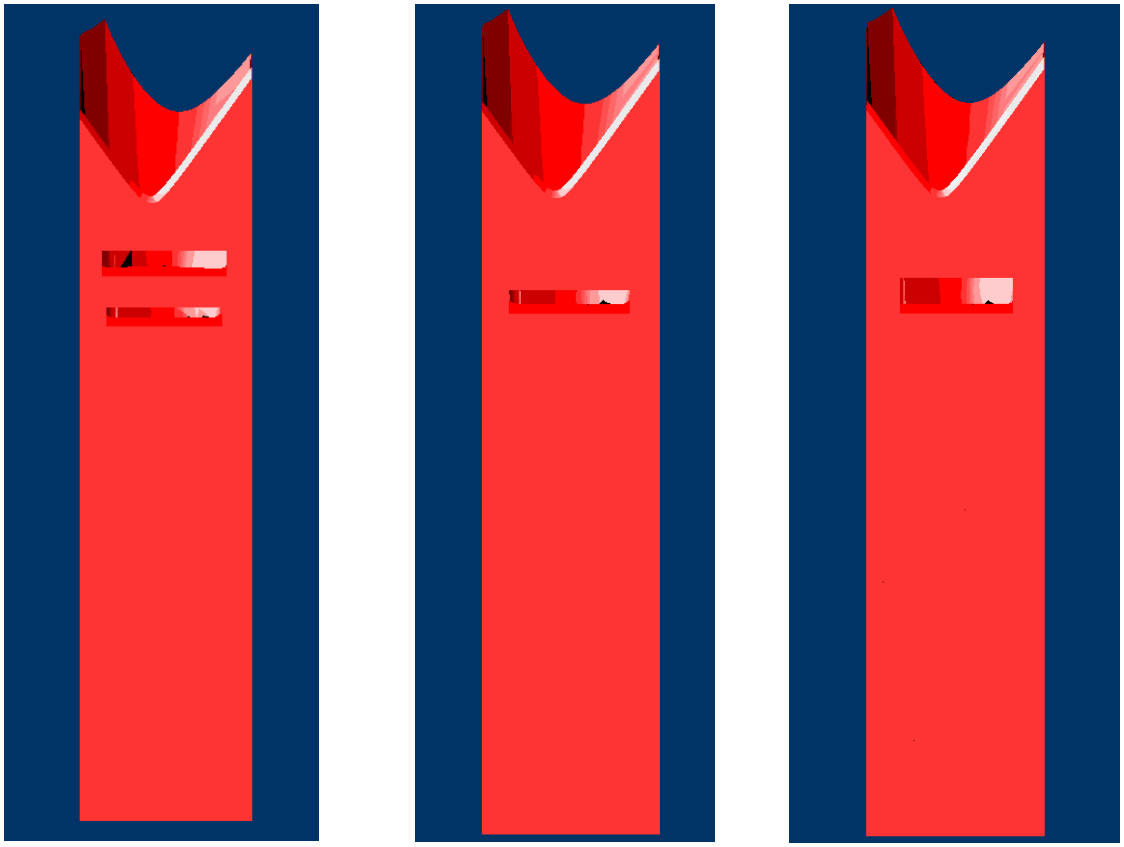

Case 4 Case 2 Case 5

Figure 10: Slot Designs, Bottom Profile

Figure 11: Slot Design, Case 5 Right Side View

Slit Designs

The slit design approach was applied to two cases and, Table 3 summarizes the important design characteristics. The area required column is sized following the technique for the slot cases. These areas are included to show the justification for the assumption that the slit areas would be much greater than needed. The area designed column lists the areas generated from the slit design procedure.

Table 3. Nondimensional Slit Design Characteristics

	Crotch Location (x/L)	**Angle at Crotch (deg)**	**Area Required (A/A_{max})**	**Area Designed (A/A_{max})**
Case 1	0.3278	37	0.0991	0.2401
Case 3	0.4111	30	0.2123	0.7239

Figure 12 shows the two designs, as generated in Rhinoceros, so that the designs can be compared visually.

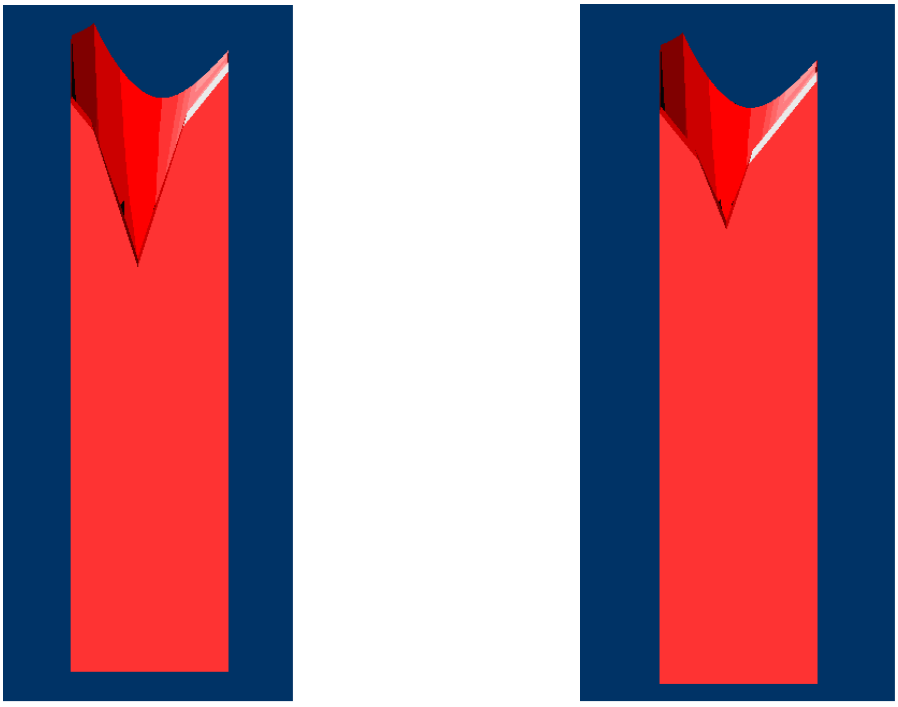

Case 4 Case 1

Figure 12: Slit Designs, Bottom Profile

IV. Numerical Simulation

Chapter Overview

The numerical simulation required the use of three computer programs; a grid generator, a solver, and an analyzer. A grid generator allows the user to import or create geometries in two or three dimensional space and generate a numerical mesh. This mesh is the computational plane that contains every point in space in which the solver will calculate the governing equations. A solver, as described above, calculates and simulates the flow, but is also the governing program which sets the problem's boundary conditions and initial conditions. The solver also sets the type of simulation, whether it is transient, steady state, or a mix of the two. The analyzer takes the large output files from the solver, and reduces the data into an easily viewable format. Since each point in the mesh has multiple outputs, i.e. pressure, temperature, Mach number, etc., the analyzer program helps simplify the information so that individual pieces of information may be observed and studied. While it is true that most solver programs come with a visualization package, they are generally limited while analyzer programs are written specifically for this task. For this thesis, Gridgen was the meshing program, CFD++ was the solver, and Tecplot was the analyzer.

Grid Generation

Gridgen is a meshing program created by Pointwise Inc. It is a highly robust meshing package that allows the generation or importing of any geometry (12). Gridgen allows for the creation of structured, unstructured, or mixed meshes. Upon completion of using the program, Gridgen has the ability to output suitable files for the grand majority

of commercial CFD solvers (12). The above traits made Gridgen a suitable application for use in this thesis.

Computer aided drafting files, created from the Rhinoceros program, could easily be imported into Gridgen. These geometries were imported as database geometries and are used by the program as reference geometries. The Rhinoceros files contain more information concerning the geometries and reference points than is needed in the grid mesh, so the database file allows the user to decide which geometries are most useful and declare them as connectors and surfaces. Connectors are the base unit in Gridgen, and along any connector one must assign a dimension. This dimension tells the mesh how many data points are along the line. This information along with the dimension of all other connectors is what allows the mesh to be created.

With the proper connectors assigned to the desired databases, one must create domains in order to establish surfaces and boundaries. A domain is created by linking connectors until they make a closed surface. It is similar to choosing the four sides of a square or the arcs of a circle. Once the surface is chosen, the package uses the dimensions of the connectors in order to create a mesh of internal points in the domain. Further accuracy of the model can be assured by using the proper connectors and the surface database. With these connectors defined and the surface database, Gridgen can lay the domain on the database surface. Otherwise, without a database surface, Gridgen will use a numerical solver in order to best estimate the surface.

Domains can also be created in two methods; structured and unstructured. Structured domains will be highly organized and square like the stringing of a tennis racket. Unstructured grids will attempt to fill the domain with triangles or other

geometries of a user specified size. The structured method requires an exact equivalency in dimension on each side of the domain in order to successfully create a grid. This is excellent for simple geometries with similar sizes, but highly complex shapes and sizes favor the unstructured. Unstructured domains were used in the numerical modeling of the Mustang II inlet because of its complex geometries.

After the completion of the domains, a block can be created. A block is the unit in which the CFD solver will run its simulation. A block is a grouping of domains such that it makes an enclosed volume. Since unstructured domains were chosen for the domains, the blocks will also be unstructured as the mesh software will fill the volume with pyramids, tetrahedral, and other three dimensional shapes.

The Mustang II inlet, in general, was broken into two blocks. The first block contained the stream tube through the inlet, and the second block contained the flow around the inlet. Other blocks had to be created for the slot cases where the slots through the inlet became a block. The meshes for the modeled Mustang II inlets had the following characteristics, as seen in Table 4, and an example of the grids created can be seen in Figures 13 and 14.

Table 4. Mesh Characteristics

	Connectors	**Domains**	**# of Blocks**	**Points in Blocks**
Case 1	111	40	2	2264955
Case 2	128	45	3	2578080
Case 3	113	41	2	2424742
Case 4	151	55	4	2497467
Case 5	157	58	3	2519907

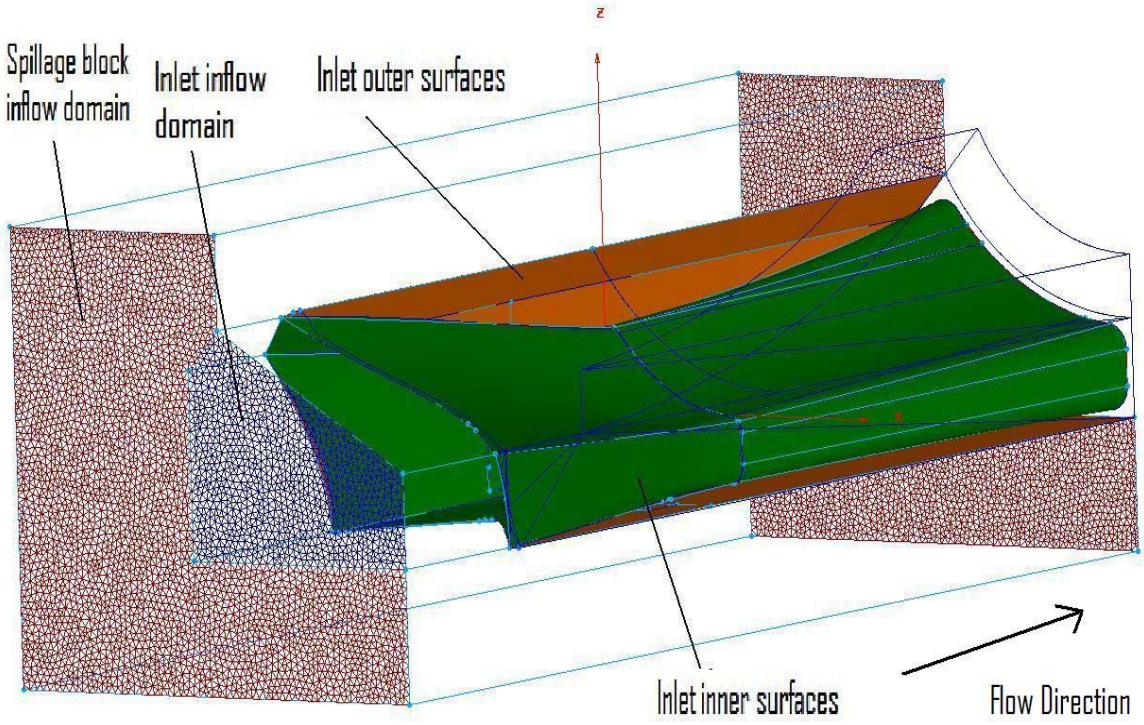

Figure 13: Example of Created Domains and Blocks, Inflow Portrait

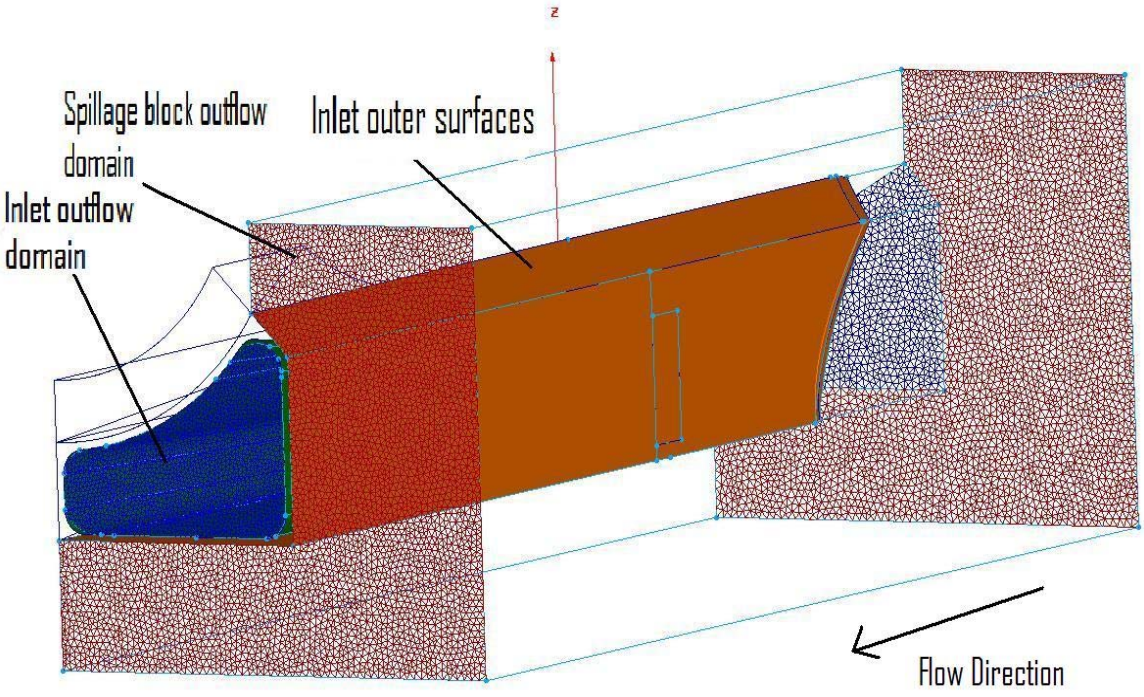

Figure 14: Example of Created Domains and Blocks, Outflow Portrait

The light blue lines in Figures 13 and 14 represent the connectors. The dark blue lines are database lines that were imported but not included in the computational domain. The inlet was designed to spill out away from the missile body (9), hence the spillage block is the area away from the curved portion of the inlet where the missile body would sit. The dark blue meshed domains, in Figures 13 and 14, are the inflow and outflow domains for the inlet stream tube block. The red meshed domains are the inflow and outflow domains for the spillage block.

CFD++ simulation

The simulation of the five cases and the two non-modified inlet base cases required two phases. First a steady-state inviscid analysis was run with a wall boundary condition at the back of the inlet to simulate the boost phase of the missile. This would simulate the large standing shock in front of the inlet that must be swallowed when the inlet attempts to start. Second, the wall would be removed and replaced by a simple back pressure in an inviscid transient analysis. The simple back pressure is used in order to simulate the backpressure imposed upon the inlet by the turning and combustor sections located behind the diffuser. As stated above, the resulting analysis would be an inviscid, transient simulation and the time step is an important factor in transient simulations.

The initial conditions for each case are set by the properties in the case. CFD++ has an interview process for the initial condition specification, and it only needed the case altitude and Mach number in order to set all of the initial conditions. These values were used in the initial steady-state simulation as a starting point. The results from the steady-

state solution were the initial conditions for the transient analysis. Table 5 lists the initial conditions given to each case.

Table 5. Initial Conditions

	Altitude	**Mach Number**	**Pressure (Pa)**	**Velocity (m/s)**	**Temperature (^{o}K)**
Base 1	10 km	2.7	26499	808.82	223.25
Base 2	1 km	2	89876	673.02	281.65
Case 1	10 km	2.7	26499	808.82	223.25
Case 2	10 km	2.7	26499	808.82	223.25
Case 3	1 km	2	89876	673.02	281.65
Case 4	1 km	2	89876	673.02	281.65
Case 5	10 km	2.7	26499	808.82	223.25

The boundary conditions were similar for all of the cases. The boundary conditions were shared by each case except for the back pressure imposition in the transient analysis. The following is a description of the boundary conditions chosen, and their relative impact upon the numerical simulation.

- Supersonic Inflow – This condition sets the flow direction and speed at the desired Mach number. Flow is only allowed to enter the volume, so the boundary must be sufficiently far from the inlet to ensure the proper creation of the standing shock.
- Characteristic Based Outflow - This condition allows the user to put no restriction on the outflow and have the outflow solely calculated by interior points. This BC was chosen for the flow leaving the block opposite of the inflow condition and outside of the inlet.
- Characteristic Based Inflow/Outflow – This BC was chosen for the sides of the block where spillage from the inlet and effects of the standing shocks

may cause flow to leave/enter the volume. This BC was given to the sides of the block parallel to the flow direction. It is based on interior point calculations and the given initial conditions.

- Inviscid Wall – This condition simulates the physical surfaces of the inlet, but does not affect the flow with viscous forces. These walls do simulate the pressure rise that would occur due to the inlet contraction ratio.
- Symmetry – This condition exists between two blocks where the blocks share a common domain. This condition allows the two blocks to compare and exchange information to ensure equal results at the boundary for both blocks.
- Simple Backpressure – This BC was only used in the transient case and allowed for the imposition of a backpressure for the exiting flow. This BC attempted to meet the user specified pressure by changing properties of the flow near the condition.

Figure 15 shows were each of these boundary conditions were applied to the imported grid.

Table 6 is a list of the backpressure used in the transient cases. These values were chosen because they are values higher than the free stream, but lower than pressure experienced once the combustor has ignited (9).

Table 6. Backpressure used in Transient Analysis

	Pressure, (Pa)
Case 1	90,000
Case 2	90,000
Case 3	100,000
Case 4	100,000
Case 5	90,000

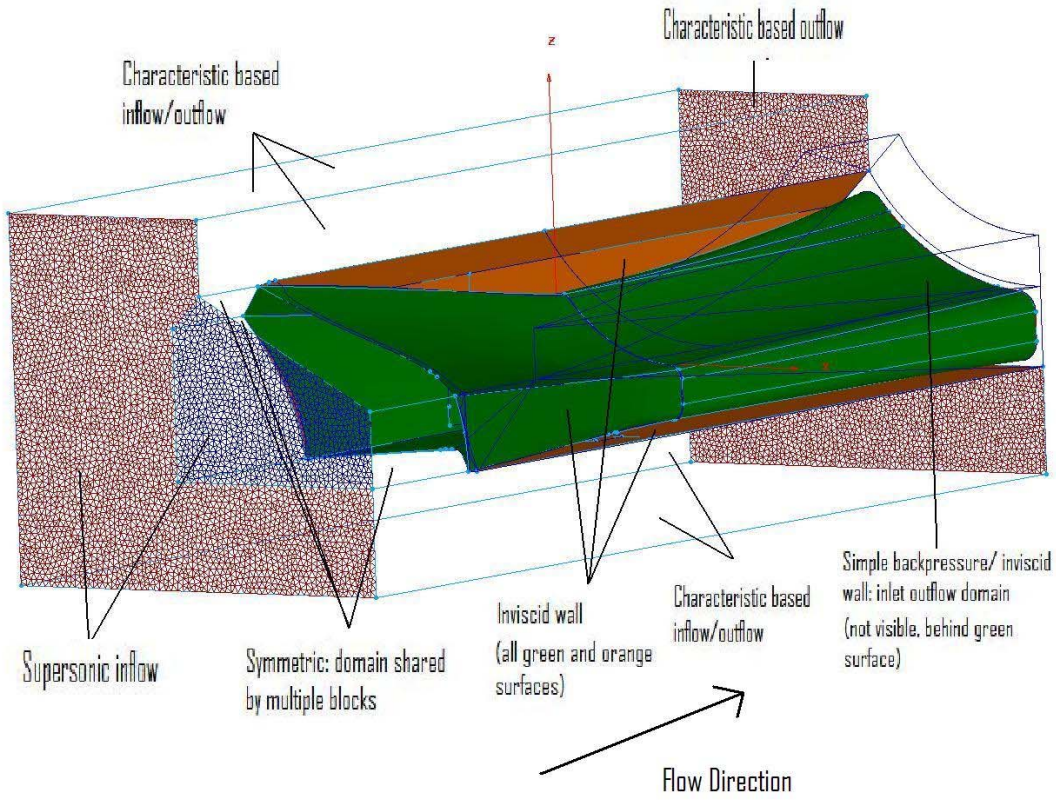

Figure 15: Location of Boundary Conditions on the Imported Grid

The transient analysis is highly dependent upon time step. While any time step can be chosen, one must be careful to ensure the stability of the solution while also

keeping the required time to calculate at a minimum. One can choose a time step by analyzing two major factors; the physical time scale and the computational stability.

The physical scale is inherent to the problem and open to interpretation by the user. One physical scale could be the length of the inlet or its width. Since the major factor in this problem was the need for the shock to move down the inlet, a time scale could be set as the distance from the standing shock to the inlet exit divided by the upstream velocity. A time step can be derived from the time scale by estimating how many steps one wants to achieve during the flow through the inlet. Mark Hagenmaier, an advisor from AFRL, suggested that for a problem of this physical size, one hundred steps would be appropriate (9). Therefore a time step could be defined as follows in Eq. (5),

$$\delta_t = \frac{\frac{L}{U}}{100} \tag{5}$$

The computational stability is rooted in the eigenvalues of the problem. During the steady state simulation, CFD++ outputs the eigenvalues of the problem. A time step can be generated by saying that one needs the time step times the eigenvalue to be less than a specified number in order to hold stability. Generally, according to Dr. Hagenmaier, this number is around one hundred for problems of this type, scale, and numerical scheme used by CFD++ (9). An equation for the time step based on eigenvalues is shown in Eq. 6,

$$\delta_t = \frac{100}{\lambda} \tag{6}$$

The results from the above time step calculations are given in Table 7. The results show that velocity is a large influence upon time step. Therefore the cases with similar

Mach numbers had similar time steps. Overall, the eigenvalue method gave the most conservative time step. A time step near the physical time scale was used after initial experimentation with the time step and discussion with Dr. Hagenmaier (9).

Table 7. Time Step Calculations (sec)

	Physical Time Scale	**Eigenvalue Time scale**	**Chosen Time Scale**
Case 1	6e-6	11e-6	4e-6
Case 2	6e-6	4.6177e-8	4e-6
Case 3	8e-6	8.0e-8	8e-7
Case 4	8e-6	9.3448e-8	8e-7
Case 5	6e-6	15e-6	1e-6

Equally important to the choice of time step is the designation of the governing equations used to solve the simulation. Since these cases were all simulated with the inviscid assumption, CFD++ used the conservation of mass, momentum (three equations), and energy in order to simulate the system (4). These equations are also known as the inviscid, compressible, perfect gas Navier-Stokes/Euler equations and are presented in general form in Eq. (7 – 9) (14),

Mass: $$\frac{\partial \rho}{\partial t} + \frac{\partial}{\partial x_i}\left(\rho u_i\right) = 0 \tag{7}$$

Momentum: $$\frac{\partial}{\partial t}\left(\rho u_i\right) + \frac{\partial}{\partial x_j}\left(\rho u_i u_j\right) = -\frac{\partial p}{\partial x_i} + \rho g_i + F_i \tag{8}$$

Energy: $$\frac{\partial}{\partial t}\left(\rho c_p T\right) + \frac{\partial}{\partial x_j}\left(\rho c_p u_j T\right) = \beta\left(\frac{\partial p}{\partial t} + u_j \frac{\partial p}{\partial x_j}\right) + \frac{\partial}{\partial x_j}\left(\Lambda \frac{\partial T}{\partial x_j}\right) \tag{9}$$

The transient analysis would also call for the use of other equations in order to assure the stability of the solution as it progressed through the transient analysis. The external aero tool in CFD++ assisted in setting all of the proper equations and included a

Riemann solver to assist transient, supersonic analysis with strong shocks (4). The tool also defined a range of Courant numbers, an analysis variable used to ensure the stability of a time step, which fit the given Mach numbers and analysis type (4). The chosen transient simulations utilized an implicit integration with dual time-stepping (dual time-stepping is required for a transient analysis in CFD++) (4).

Once the simulations were properly established they could be physically run on a computer system. The system used in this thesis was the Aeronautical Systems Center Major Shared Resource Center (ASC MSRC) and all of the following information was obtained from reference 1. The ASC MSRC has four main computing nodes; SGI Origin 3900 (hpc11), COMPAQ SC-45 (hpc9 and hpc10), COMPAQ SC-40 (hpc5), and SciVis (svw10 and svw11). While all four clusters were available for use, hpc11 was chosen because of Dr. Hagenmaier's knowledge and familiarity of that system. The SGI Origin 3900 contains 2028 processors with a 2.9 Peak TeraFLOPS capability. Each processor has 1 gigabyte of memory and a total workspace capacity of 25.5 terabytes. Tape archives are also available. The operating system for the hpc11 node is IRIX UNIX. Direct terminal access was available at the ASC facility, but remote login was the preferred access method. A local Linux machine of the AFIT network could access one of three UNIX machines on the AFIT Network; Nordic was the UNIX machine used most often. A Kerberos shell could then be initiated and a ticket could be obtained for access to the hpc11 system. All hpc11 programs and drives could then be accessed on the local Linux machine.

Data Reduction

The results from CFD++ were analyzed using Tecplot; a commercially available program with extensive tools designed to help CFD post-processing. Capable of loading multiple databases at once and producing two and three dimensional plots, Tecplot easily proved itself to be a more capable post-processor than the CFD++ visualization tool. Specifically, Tecplot was used to create slices through the data field in order to see patterns and trends for all of the results from the analysis including pressure, temperature, and Mach number. These slices could then be viewed individually or multiple slices could be made into a movie in order to see how the trends changed over time.

V. Results and Discussion

Results

Initial examination of the results showed that a slice down the middle of the inlet could be characterized as an average result for the entire inlet. Figure 16 shows four slices through Case Base 1. The X value given for each slice reveals the X-plane of the slice through the inlet. As can be referenced from Figure 18, which also shows a slice of Case Base 1 with X = -0.06, the right wall of the computational block is referenced as X = 0. Therefore as X becomes more negative, one is moving to the left through the computational block.

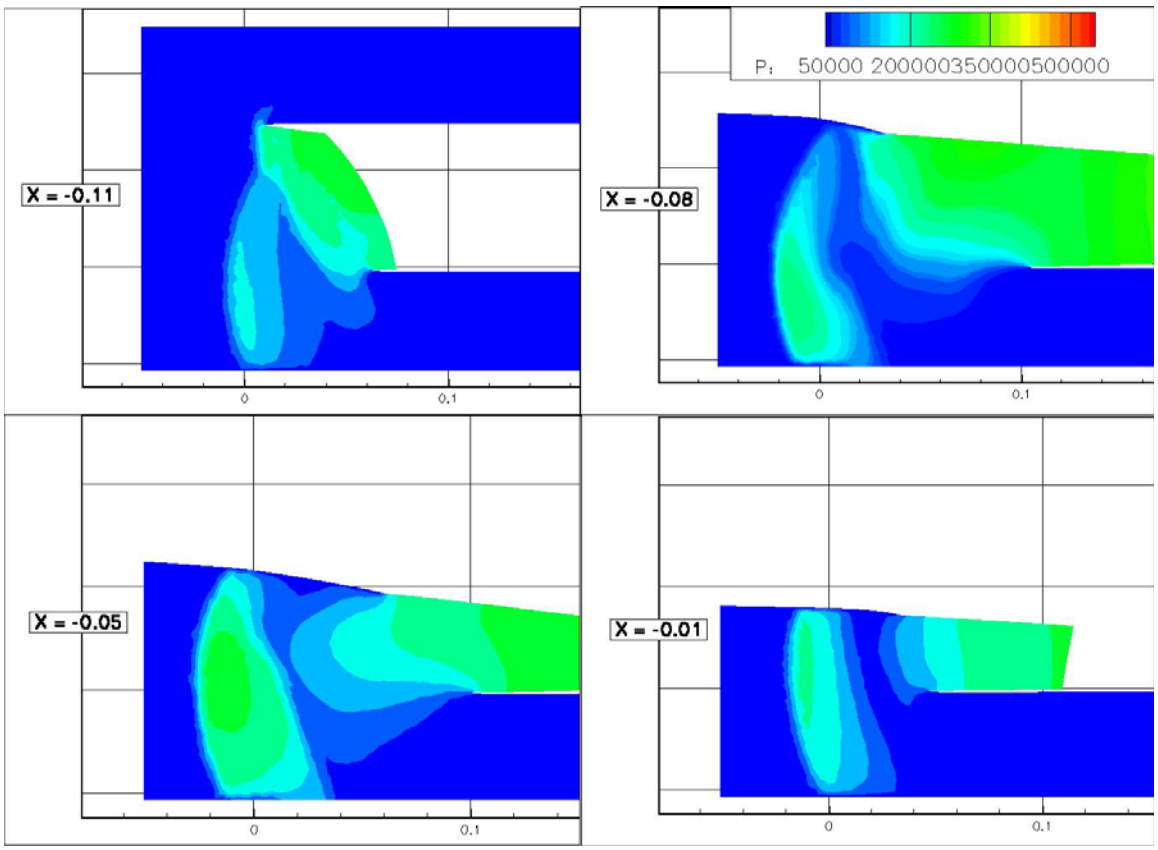

Figure 16: Four Pressure Contour Cross Sections of the Case Base 1 in the Indicated X-plane.

The standing shock, the quick change in color representing a change from a pressure of 5,000 Pa to approximately 325,000 Pa, seen in Figures 16 does change position because of the complex three dimensional geometry of the inlet. However, an average of the four slices, and hence represented in Figures 17 and 18, show that for an average the shock does not change significant 'Y' position through different slices of the inlet. Figures 17 and 18 are representations of a Case Base 1 slice at X = -0.06 in three dimensional space in order to give context to the slice and shock wave position in reference to the inlets physical shape.

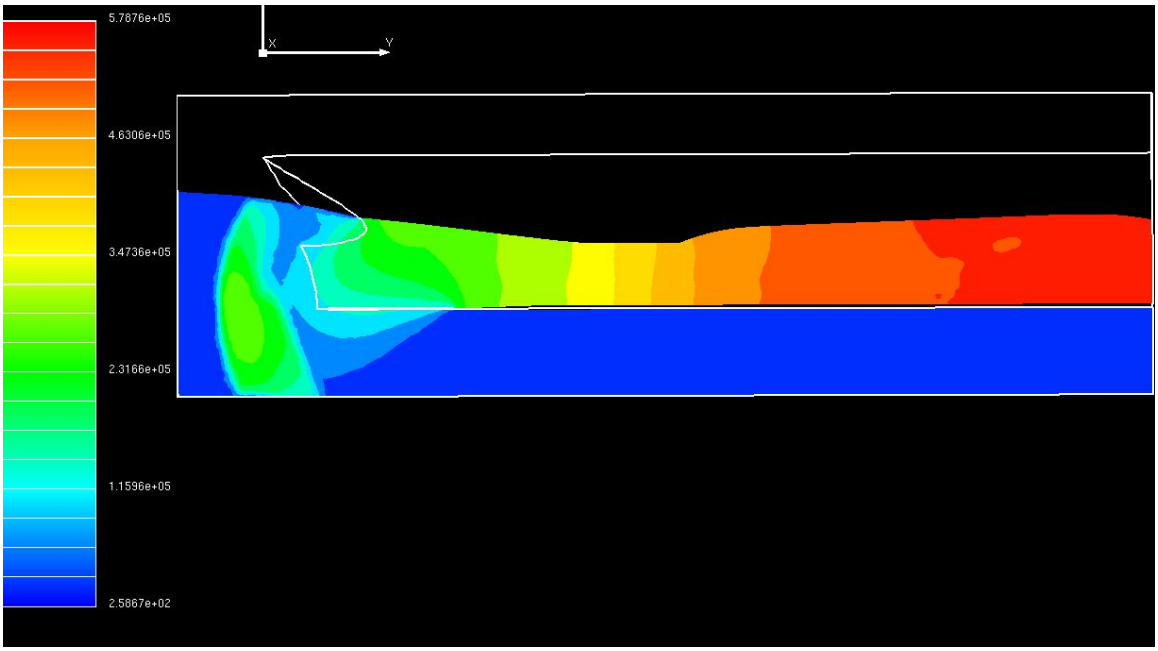

Figure 17: Case Base 1 Pressure Contours with the Inlet Boundaries. Flow Direction is Left to Right.

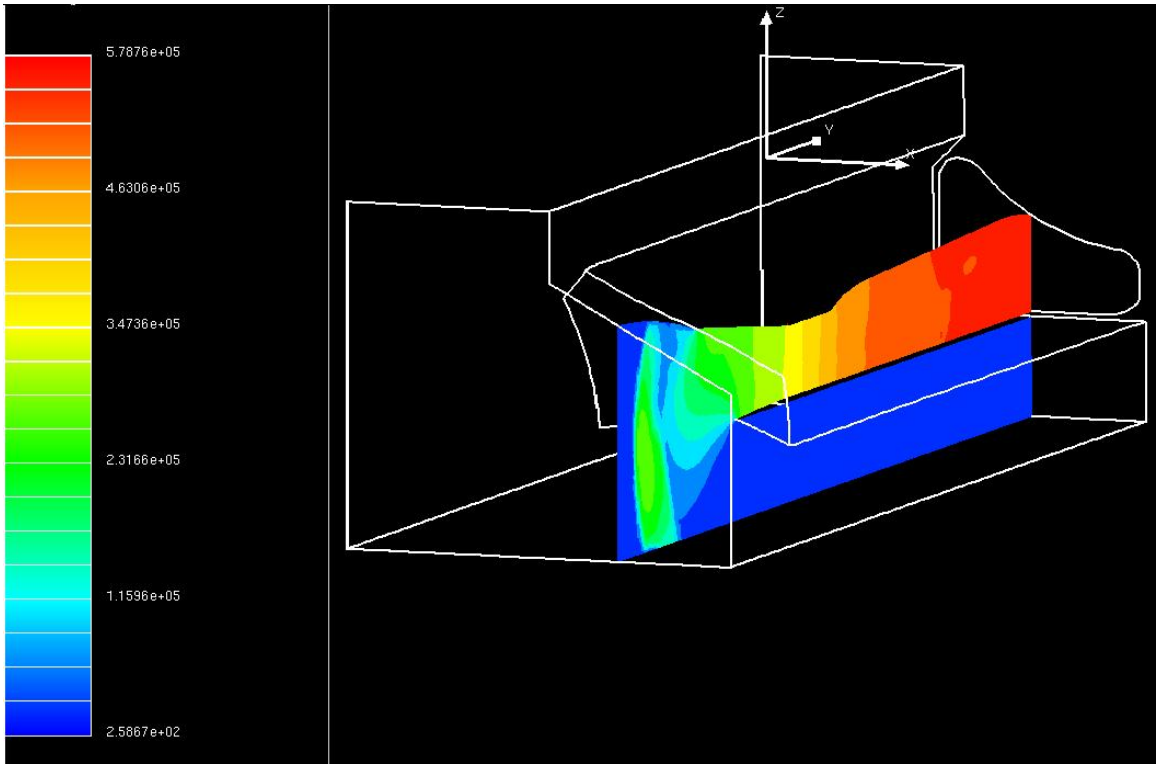

Figure 18: Case Base 1 Pressure Contours, 3-D View to Show Slice Relation to the Inlet.

The Cases Base 1 and 2 were modeled at the same time that Case 5 was simulated. It is presented first to allow for comparison between the non-modified inlet and all of the designed geometries. Cases Base 1 and Base 2 were only simulated to the conclusion of the steady-state simulation. The results of those simulations are plotted in Figures 19 and 20 and show the pressure and Mach number contours through the inlet slices. The flow direction in Figures 19 - 30 is moving left to right. Figures 19 and 20 are also related to Figure 17 and 18 by showing where significant inlet positions are located for the slices at X = -0.06. The specified slice positions are similar for Figures 21 - 30. The standing shock is also identified so that shock waves can be identified in the figures.

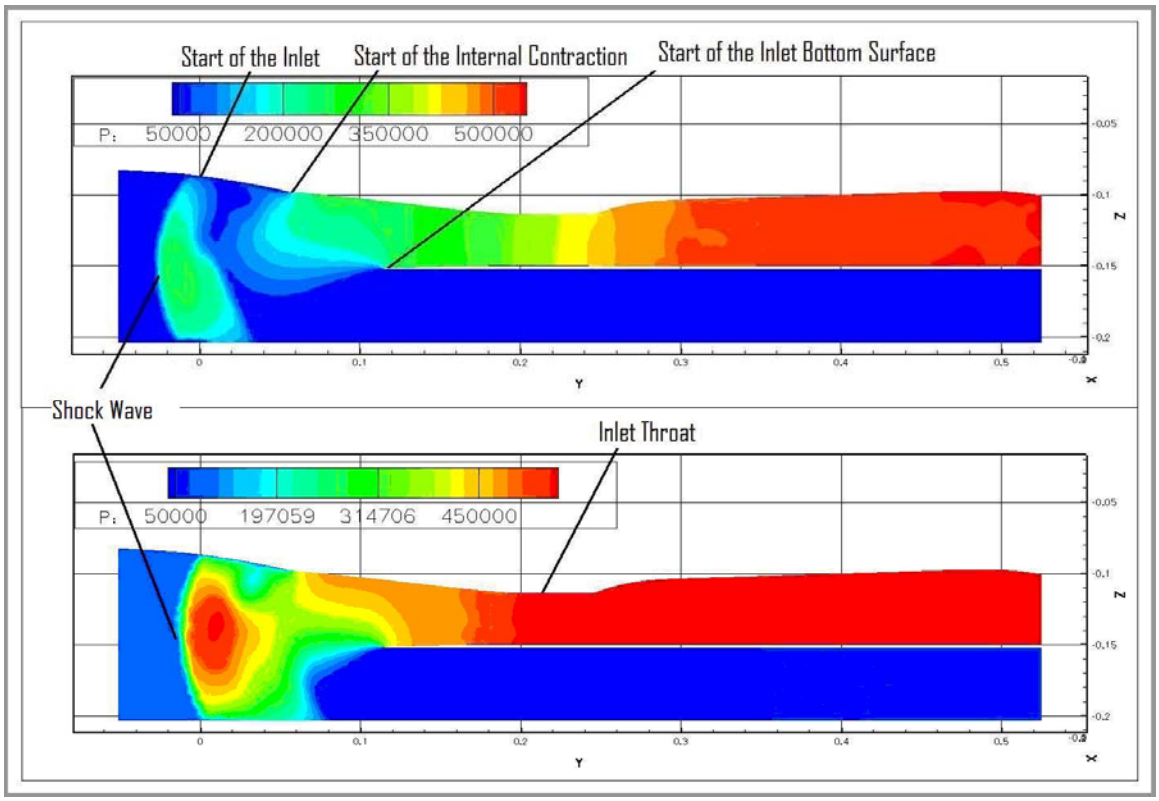

Figure 19: Pressure Contours. Top Slice, Case Base 1. Bottom Slice, Case Base 2.

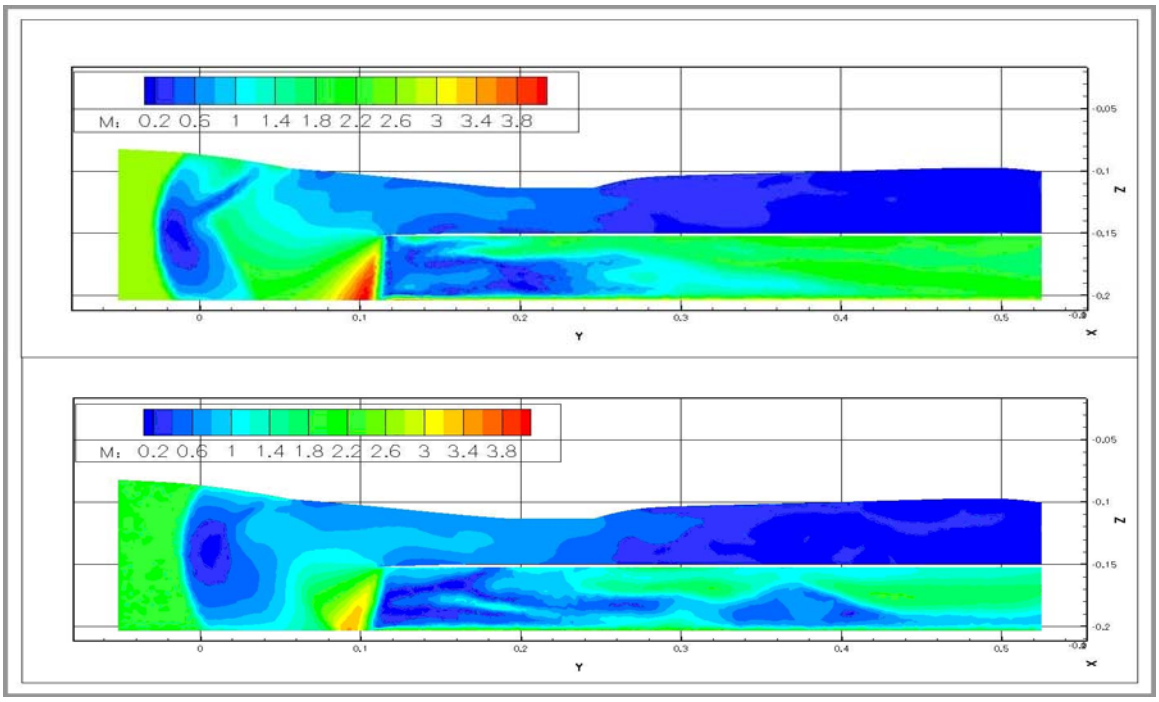

Figure 20: Mach Contours. Top Slice, Case Base 1. Bottom Slice, Case Base 2.

Cases 1 – 4 were run simultaneously, while Case 5 and the Base cases were created and simulated after those runs. The steady-state solution was run until there was no noticeable change in shock wave position for 200 iterations, and the transient solution was run until there was no change in shock wave position for 200 iterations. Figures 21 - 30 show the pressure and Mach number contours through the inlet at the middle slice for each of the cases. These figures show the contours in the inlet at the beginning of the transient analysis, time equal to zero, and at the time decided to be the steady state solution of the transient analysis. The ending times for each of the cases are given in Table 8. Since the Cases Base 1 and 2 were not run through a transient analysis, they are not included in the table.

Table 8: Ending Time and Iteration Step for Each Case

Case	**Time at last iteration (sec)**	**Iteration Step**
1	0.0162	3450
2	0.0156	3140
3	0.0056	3100
4	0.0052	3060
5	0.0057	4000

Shocks are present in the figures were there is a quick change in color that would indicate large, order of magnitude changes in pressure or Mach.

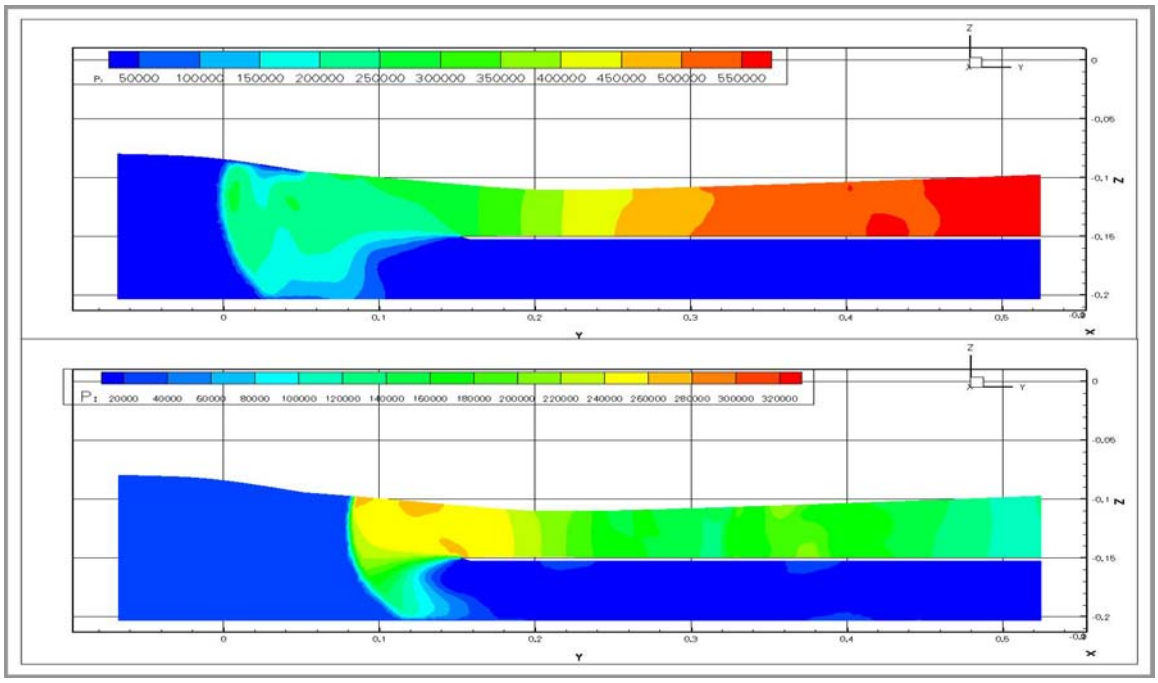

Figure 21: Case 1 Pressure Contours. Top Slice, t=0. Bottom Slice, $t=t_{final}$

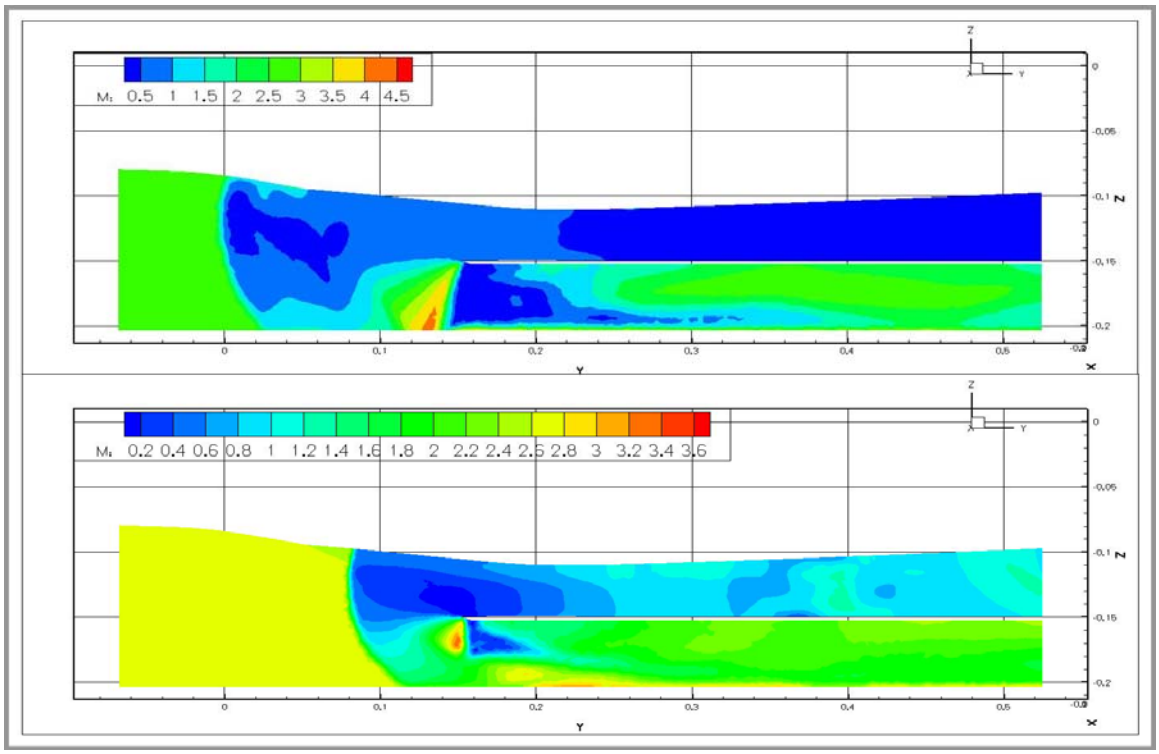

Figure 22: Case 1 Mach Number Contours. Top Slice, t=0. Bottom Slice, $t=t_{final}$

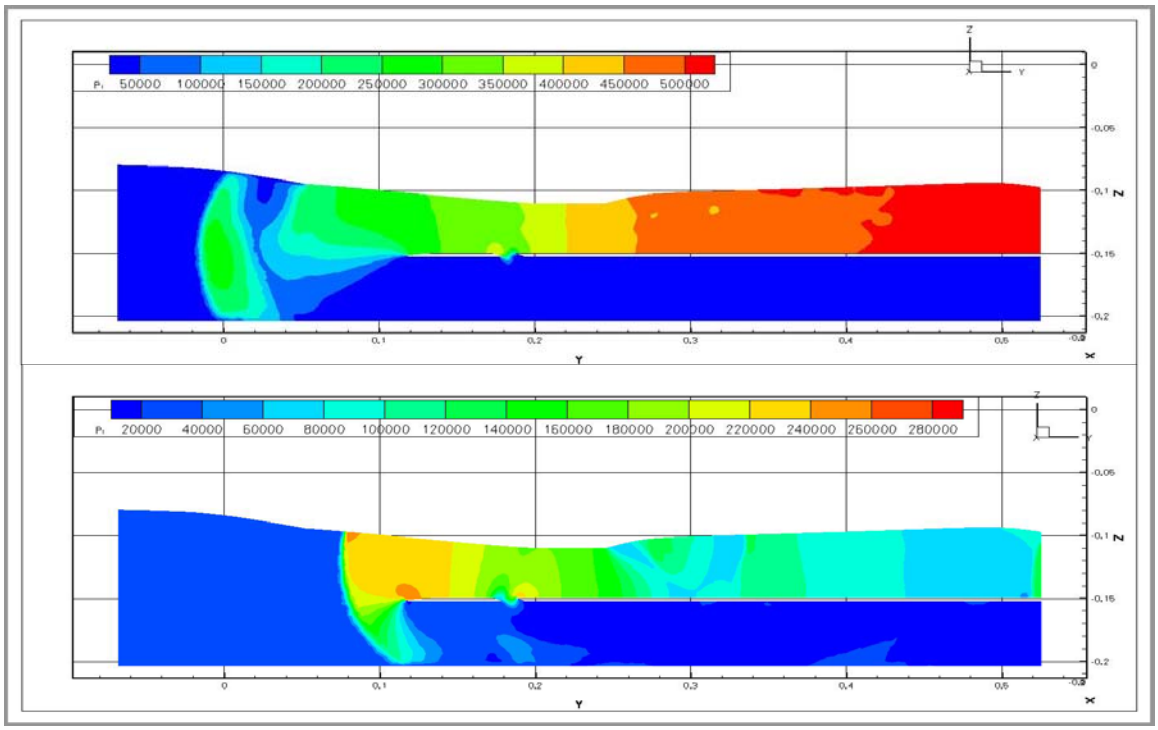

Figure 23: Case 2 Pressure Contours. Top Slice, t=0. Bottom Slice, $t=t_{final}$

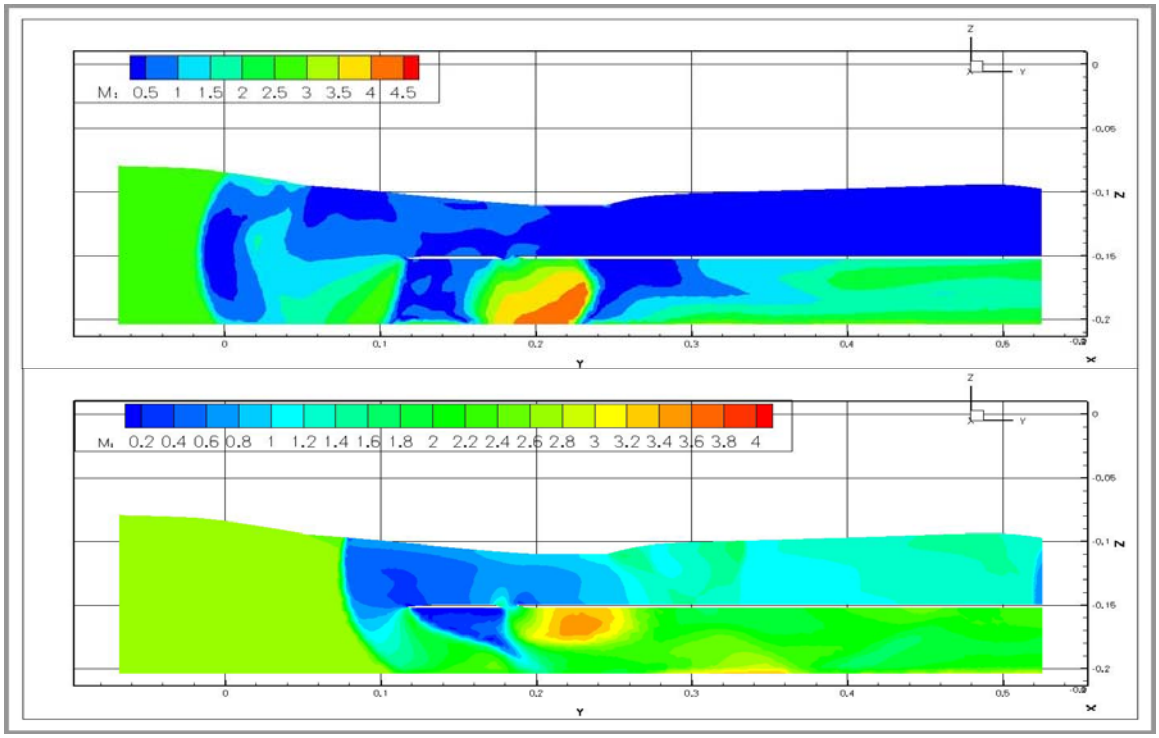

Figure 24: Case 2 Mach Number Contours. Top Slice, t=0. Bottom Slice, $t=t_{final}$

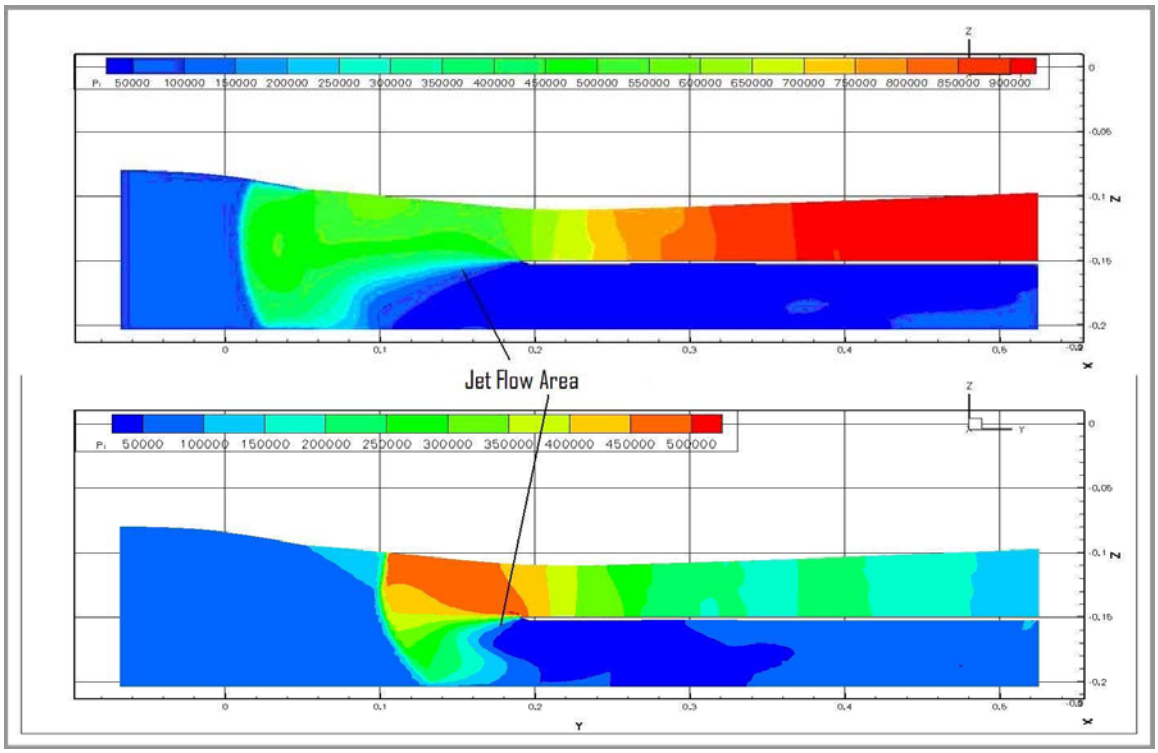

Figure 25: Case 3 Pressure Contours. Top slice, t=0. Bottom Slice, $t=t_{final}$

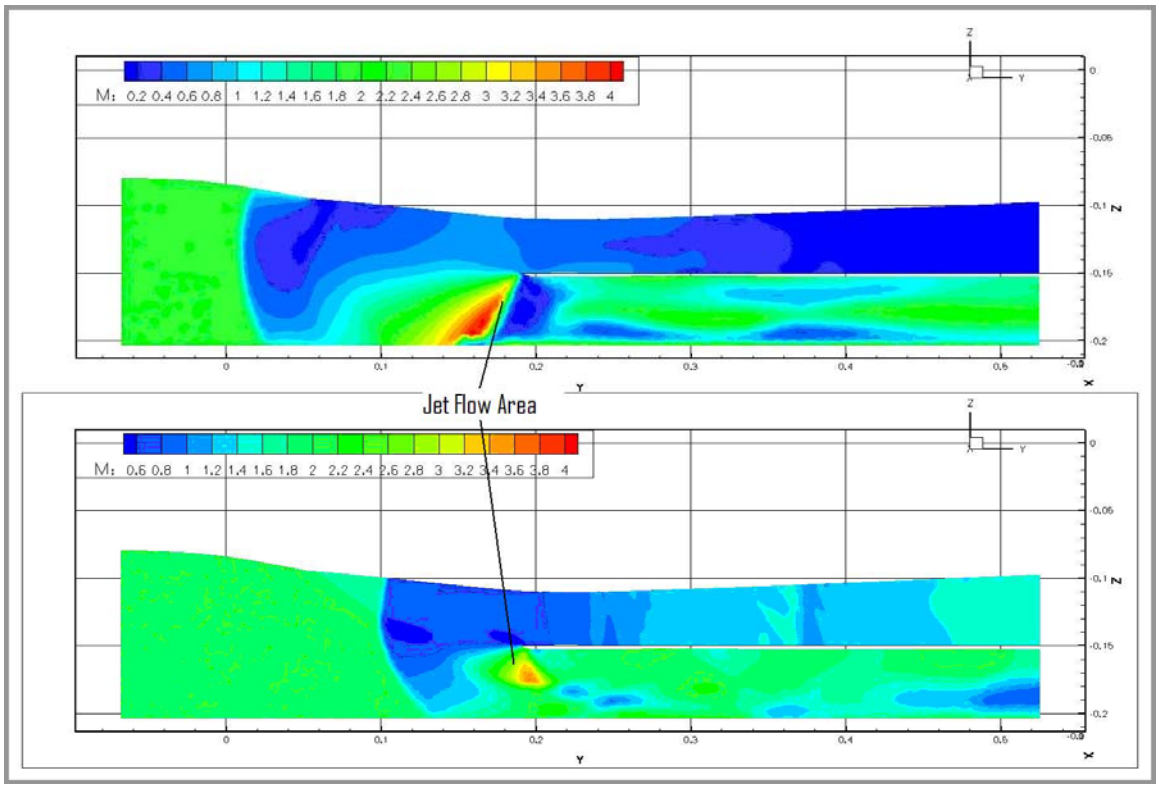

Figure 26: Case 3 Mach Number Contours. Top Slice, t=0. Bottom Slice, $t=t_{final}$

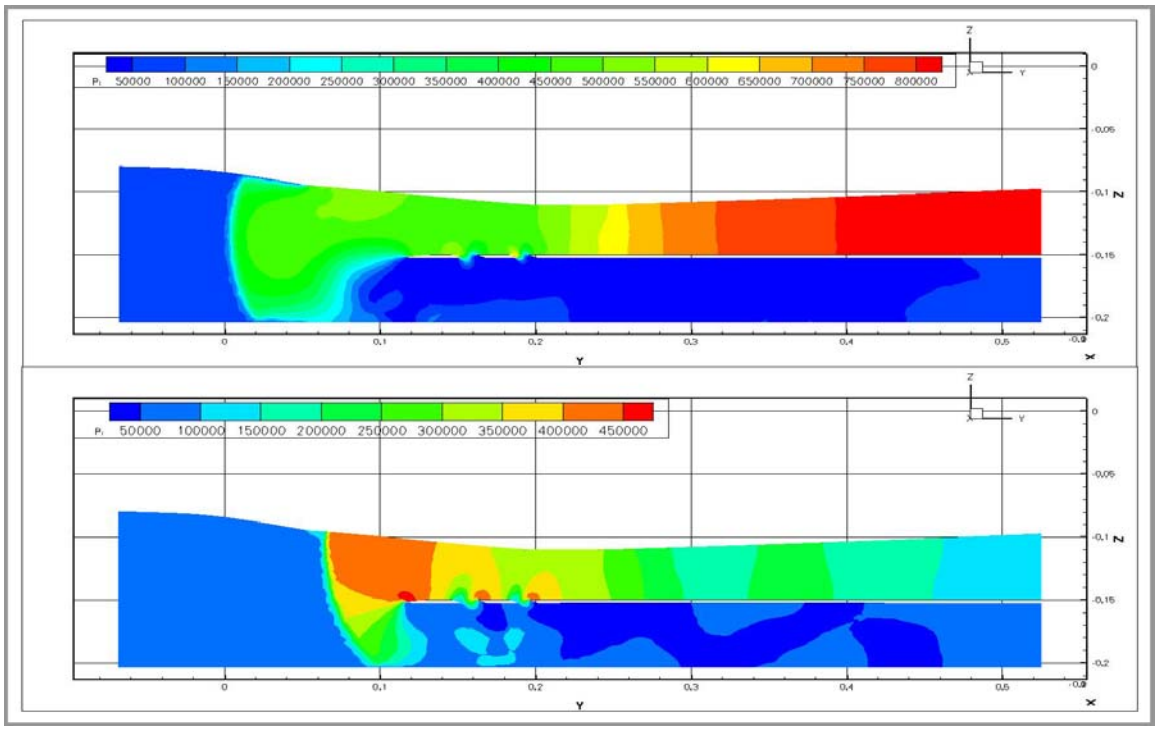

Figure 27: Case 4 Pressure Contours. Top Slice, t=0. Bottom Slice, $t=t_{final}$

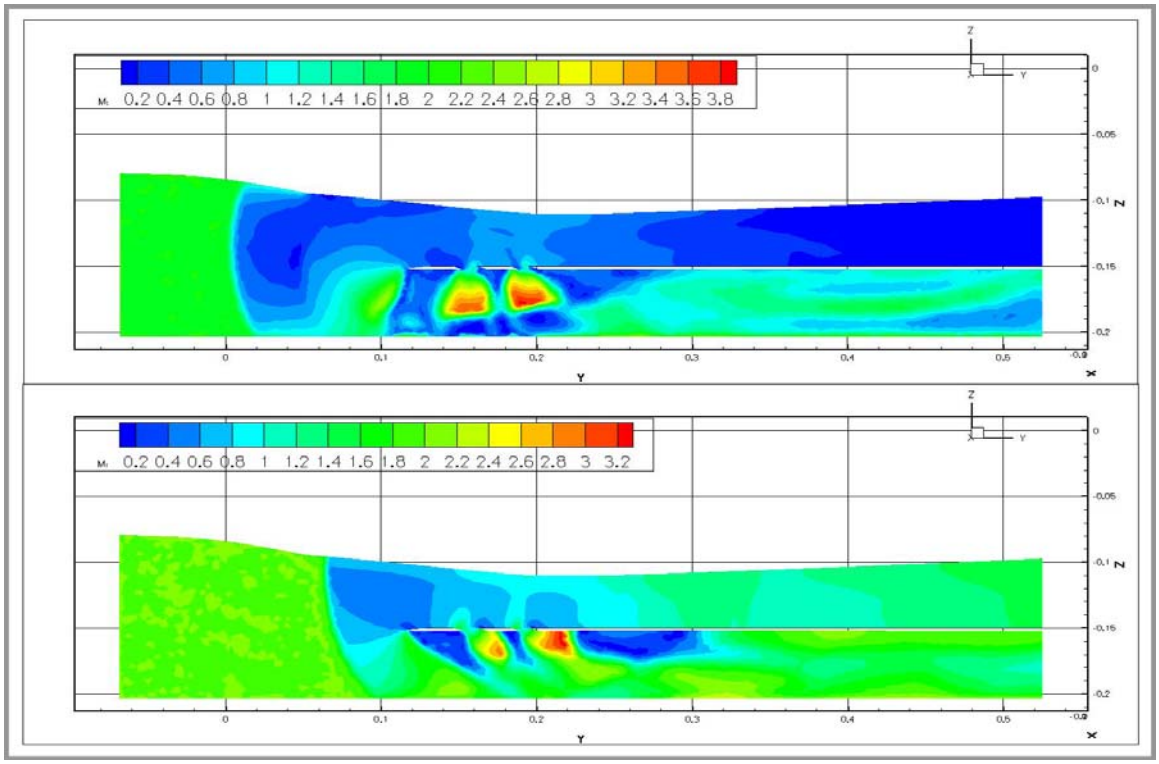

Figure 28: Case 4 Mach Number Contours. Top Slice, t=0. Bottom Slice, $t=t_{final}$

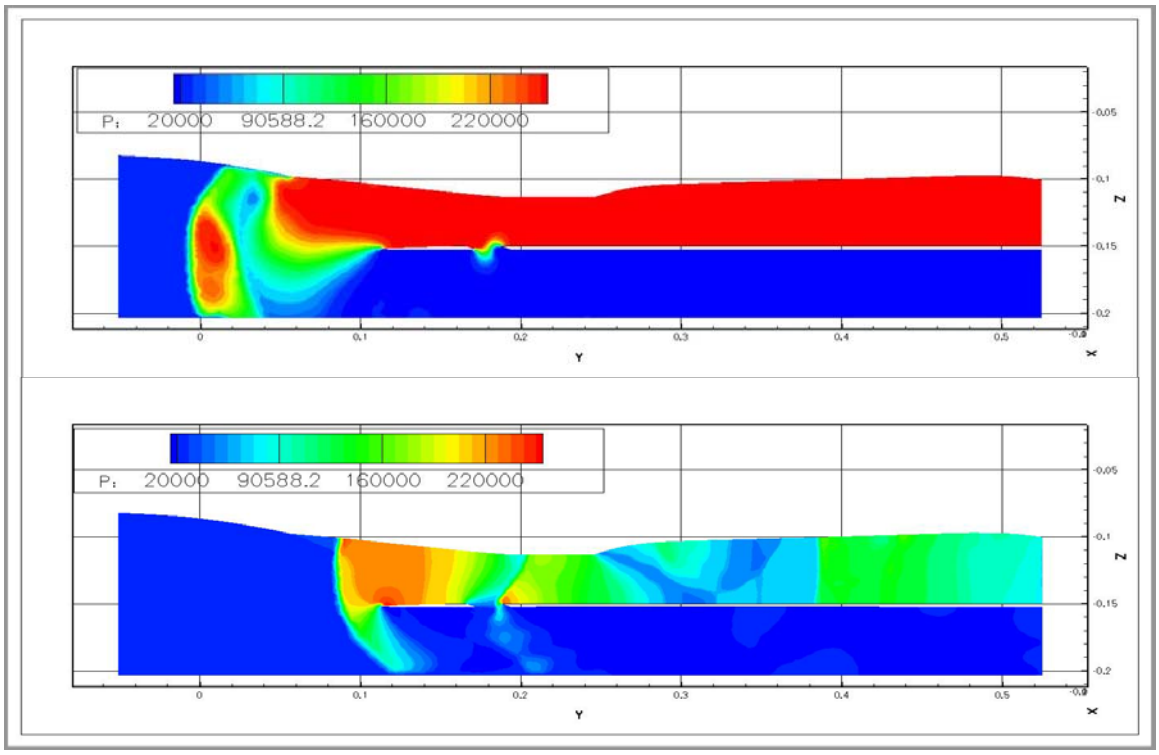

Figure 29: Case 5 Pressure Contours. Top Slice, t=0. Bottom Slice, $t=t_{final}$

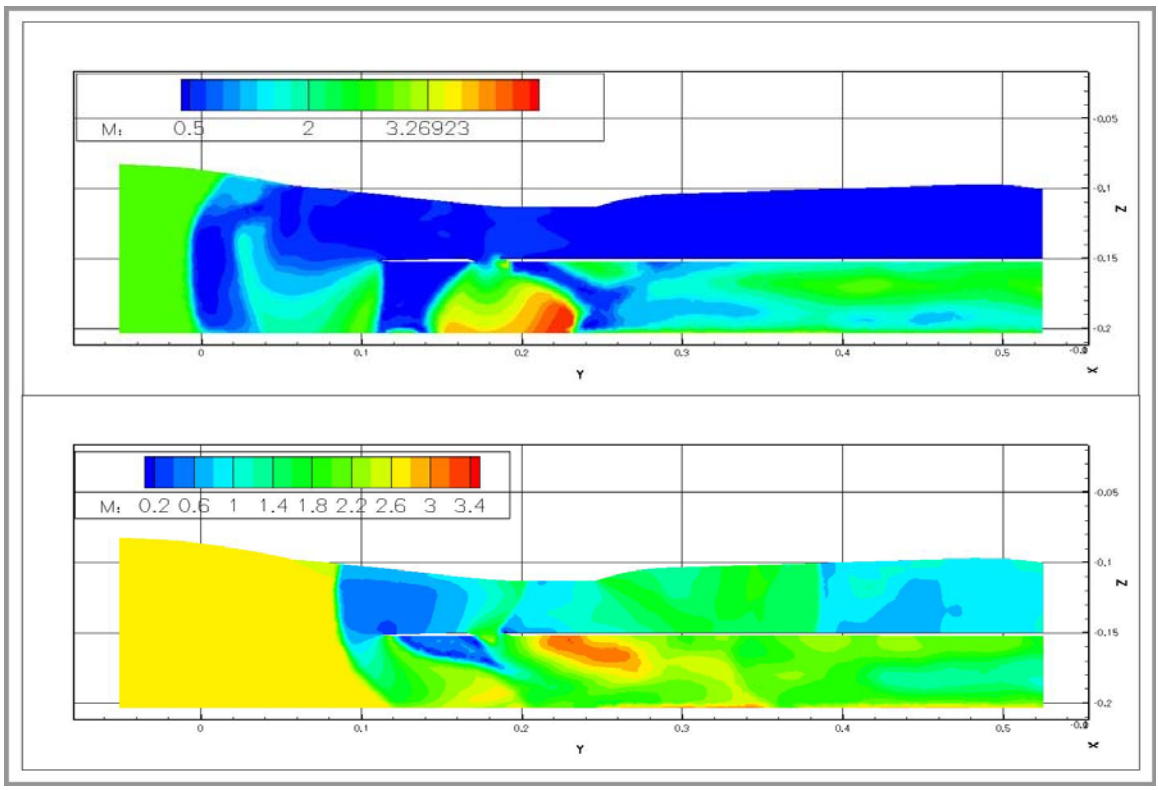

Figure 30: Case 5 Mach Number Contours. Top Slice, t=0. Bottom Slice, $t=t_{final}$

The initial and final resting places of the shock wave are presented in Table 9 for quick reference and comparison. In the table, the larger the value of Y position, the farther downstream the shock traveled.

Table 9: Initial and Final Y Position for the Shock Wave at the Conclusion of the Transient Analysis.

Case	Initial Y Position	Final Y position
Base 1	-0.03	NA
Base 2	-0.02	NA
1	0	0.08
2	-0.02	0.07
3	0.02	0.1
4	0	0.065
5	-0.01	0.08

Discussion

Cases 1 – 4

The investigation of the four cases showed that all of the cases proved to be sub-optimal as none of them were able to swallow the shock wave. At first glance, Case 3 appears to be the most successful design as the shock position is the farthest downstream at both the initial and final position. However, one can not generalize yet, that the slit design is better than the slot design, because Case 1 fairs just as well as Case 2 in terms of the final position of the standing shock. Also, since the slit designs have similar designed angles at the crotch, one could only conclude that it is the larger opening in the triangle cut near the inlet lip in Case 3 that allows the final standing shock to be at a Y position father downstream than the other cases.

In all the cases presented, the Mach number contour plot shows what appears to be a shock wave underneath the inlet at the inlet crotch, even though the pressure

contours show no such shock wave. This effect is more significant at time equal to zero, but is also present at the final time step to a lesser extent. These areas are highlighted in the Case 3 results, Figures 25 and 26, because this effect is easily viewable. These areas are not shocks, but the effects of jet flow.

If one considers the flow through the inlet at the end of the steady state analysis, there is high pressure at the back of the inlet due to the wall boundary condition. The flow in the back of the inlet wants to escape the large pressure and must travel upstream in order to exit the inlet. When this reversed flow reaches the designed slits or slots, the flow is accelerated due to the large pressure gradient and is expelled out of the inlet at a great velocity. The effect at the crotch appears because flow behind the jet is entrained and a recirculation area is created that lowers the overall Mach number. The jet flow and recirculation area is viewable on all of the results for the steady state, time equal to zero solutions, but it is most noticeable on the slit cases. The jet flow area is less apparent in the slot cases because some of the high pressure is relieved as air flows through the slots before reaching the original spill area. The Mach contours for the slots cases also reveal large bubbles underneath the slots in the steady state, and smaller angled bubbles in the transient cases. In the steady state solutions, the flow through the slots is very similar to the flow out of the spill area; downward in direction. This downward velocity direction creates the round bubbles. In the transient solutions, the areas are slanted because the flow through the slots now has a significant velocity in the streamwise direction as well as in the downward direction.

This jet flow area can be seen explicitly in a Mach number vector diagram such as Figure 31. This plot, which shows a slice at X = -0.06 for Case 3, shows not only the Mach number, but also the associated direction of the flow at that position.

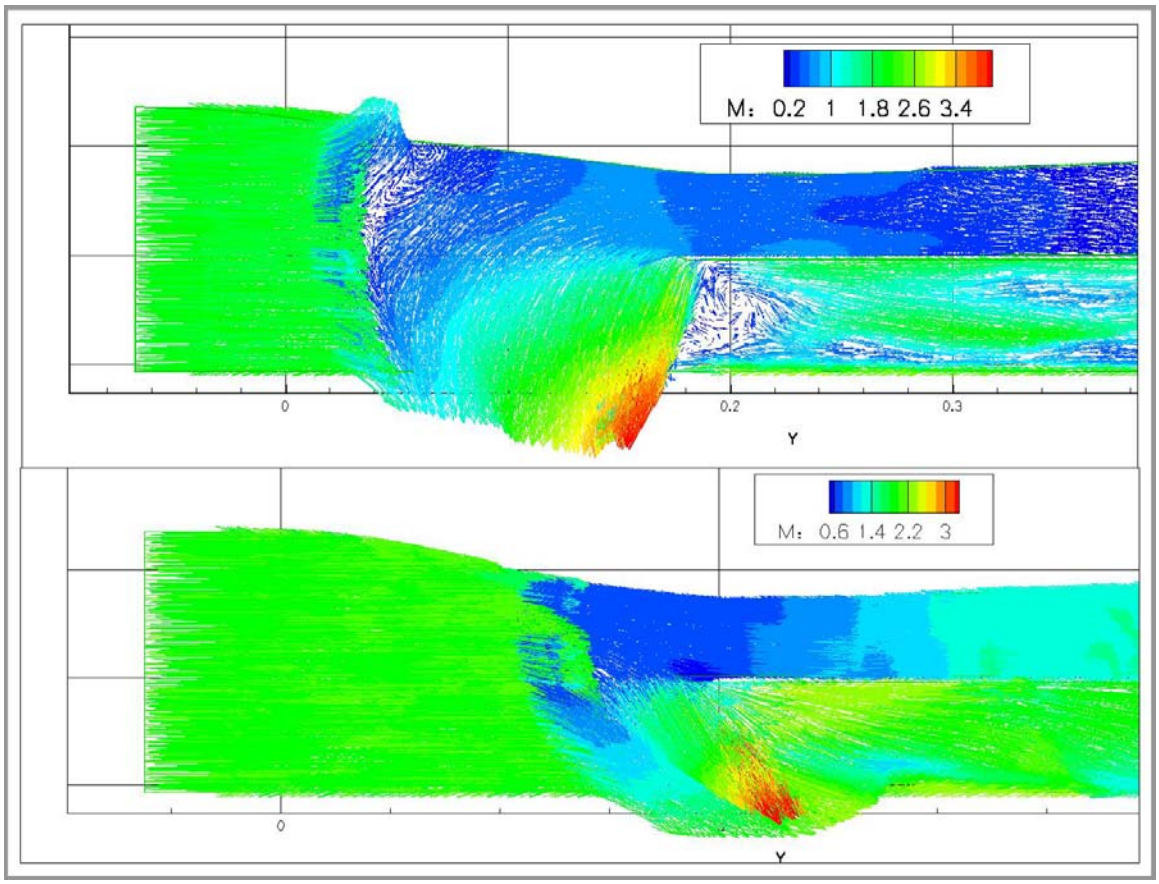

Figure 31: Case 3 Mach Number Vector Contours. Top Slice, t=0. Bottom Slice, $t=t_{final}$

Figure 31 indeed shows that there is a jet flow area in the flow field. The top slice of Figure 31 confirms that a significant portion of the flow is directed downward and that a recirculation area does develop behind the jet flow area. It also shows that the majority of the oncoming flow is directed downward, or up over the top surface of the inlet. The bottom slice validates the jet flow assumption as well, but as stated, since the flow in now

allowed to flow through the inlet, the streamwise velocity has an effect upon the jet flow and angles the flow downstream.

The results for Cases 1 and 3, the cases for the slit geometries, show that the triangular shape cut used to create the slits may not be the optimal design. With the above explanation of jet flow effects, it is obvious that at the end of the transient analysis there is still a jet flow effect. This would imply that while the slit is relieving pressure as desired, the area needs to be larger in order to be more effective. A simple way to increase the effectiveness of the slits would be to use a U or parabolic shape instead of the designed triangle shape for the slit. Further research would be needed in order to design an optimal slit geometry and design methodology.

The investigation of the slot cases, Cases 2 and 4, reveal that the bleed slots were improperly designed. One of the major assumptions made in sizing the bleed slots was the Mach number through the slots. It was assumed that the flow would be subsonic, or choked as a worst case scenario. However, Figures 24 and 28 show that the flow through the bleed slots is mostly supersonic and hence are more inefficient than previously thought. It was determined that the subsonic slots would be roughly 60% efficient, implying that 60% of the designed area must be greater than the area required from the design calculation; supersonic slots near Mach number 1.5 are approximately 25% efficient (17). Therefore, instead of increasing the bleed area by a factor of 1.6, the actual area would have to be increased by a factor of 4. Case 5 represents these design corrections.

The results show that the main assumptions, given in the Design Methodology section of this report, are valid, but they need to be augmented to account for the effects

of jet flow. The calculation of the contraction ratios assumed that the starting shock wave would not be outside of the inlet, but slightly downstream. All four cases show that the shock wave in the transient analysis does proceed downstream making this assumption valid and also shows that the free stream Mach number was a valid choice in calculating the first CR. Since all of the cases failed to swallow the shock wave, it is not possible to validate the assumption of quasi one dimensional flow. However, the significant effects of jet flow as described above cannot be neglected and should be included in the main assumptions. Use of the isentropic area contraction, Eq. (4), for changes in flow velocity inside the inlet could not be completely validates as the cases failed to swallow the shock or slow the flow.

The choice of boundary conditions has proven to be acceptable. The only areas where the boundary conditions appear to cause errors are near the characteristic based inflow/outflow conditions and at the simple backpressure. At the characteristic based inflow/outflow interfaces there appears to be a shock-bending effect. While one would expect a curved shock near the bottom of the computational domain, the solver has attempted to keep the initial conditions and bent the shock horizontally. This effect can be seen clearly in Figure 16. One would expect the shock to pass through the bottom boundary, but a solid dark blue line, implying free stream pressure, is visible implying that the solver has artificially bent the shock at the boundary. While this is an undesirable event, the effect of such bent shock waves appears to be far enough from the inlet to have little or no influence upon the inlet stream tube or designed bleed areas. The simple backpressure boundaries appear to have difficulty imposing their specified value in Cases 1 and 2. In Cases 1 and 2, the pressure appears to be higher than the given value

of 90,000 Pa. This effect may be the results of the larger time step used in cases 1 and 2, but it does not appear to have any effect as the resultant pressure is only 20,000 to 30,000 Pa above the desired value.

The overall simulation appears to be acceptable as well. While the inviscid simulation did not model viscous effects, the compressible effects due to supersonic flow are visible. While the presented results show that shock waves were formed in the flow, the figures do not show such effects as shock forming due to the inlet surfaces. Figure 32 shows Case 3 at the end of the transient analysis, and follows the same presentation as Figure 16 in terms of slice location. These cross sections show that the inviscid surfaces do indeed create weak oblique shocks waves and validate the overall simulation.

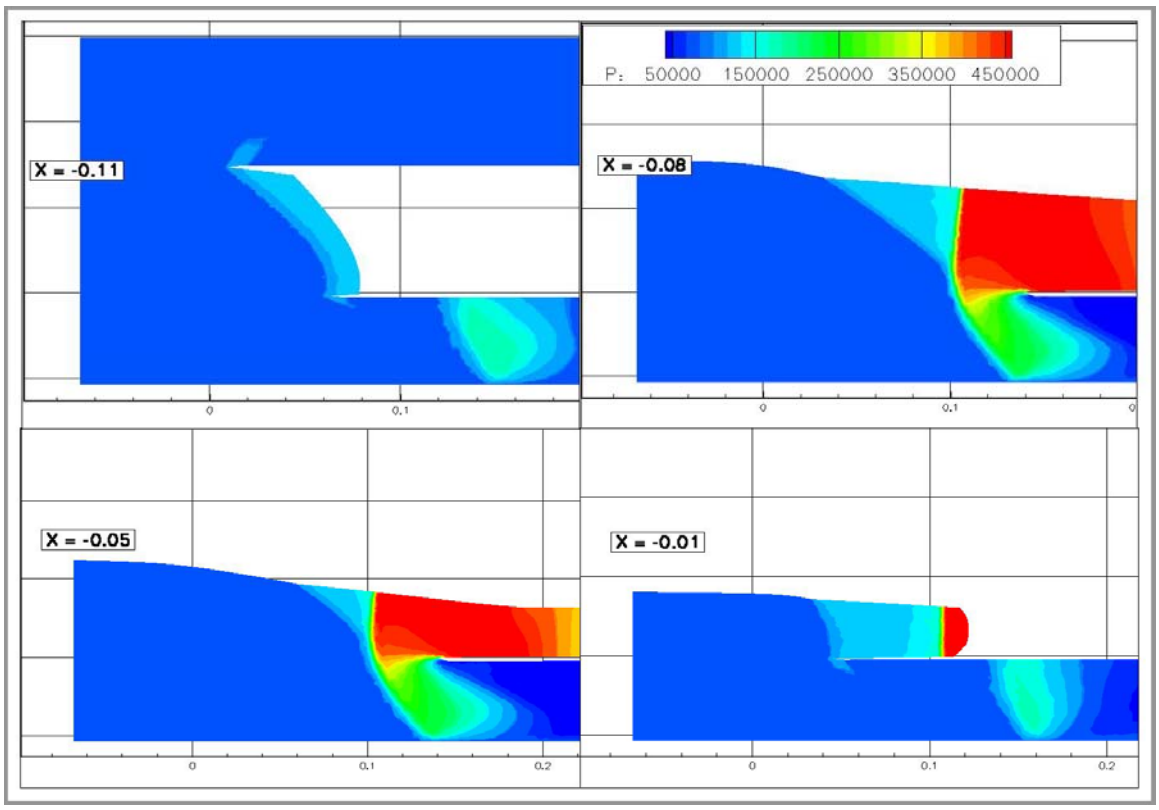

Figure 32: Four Pressure Contour Cross Sections of Case 3 in the Indicated X plane.

Case 5

The results from the investigation of Case 5 show that the modifications based upon the results from Case 2 failed to start the inlet. The results show that the modifications did not have a great impact upon the final position of the shock wave as the results only differ from the results of Case 2 by 0.01 Y units. The Mach number contour plots also show that the Mach number through the slot also increased as the size of the slot increased. These modified slots were sized assuming a Mach number of approximately 1.5, and now the Mach through the slots appears to be closer to 2. These results would imply that there is a limit to the effectiveness of slots. Another consideration would be that the slots are placed too far into the inlet. Initially, the back of the slot on the interior of the inlet was placed at the location given by the contraction ratio. A design improvement could place the back of the slot on the exterior of the inlet at the designed location. Since the slot is angled, it would move the interior location of the slot forward and may improve the overall effectiveness of the slot and reduce the Mach number through the slot as well. Another design improvement would be to place the slots on all sides of the inlet rather than limiting it to one or two of the inlet surfaces. This would alleviate pockets of high pressure in corners of the inlet opposite the sides of the slots.

Case 5 also revealed a grid flaw. In the comparison of the upper line of all of the cases, there are minor differences. These differences are due to the effect described in the numerical simulation section dealing with the creation of domains. In Cases 1 – 4, the database surfaces were not used in the creation of the domains. Therefore, even though the upper line appears to resemble the internal inlet shape, there is deviation due to

Gridgen's approximation of the surfaces. This effect was correct in the Base cases and in Case 5. This error, though, does not affect the results of this investigation discussed above. All of the observed phenomena in the first four cases were also observed in Case 5. This reoccurrence of phenomena validates the results and trends discussed for the first four cases even though there may have been slight deviations in the internal inlet shape.

VI. Conclusions and Recommendations

Conclusions

The investigation of the presented design methodologies yielded many important results that will assist in the further investigation of starting techniques for complex three dimensional inlets.

1. The slot design effectiveness was not improved when the Mach effects through the slots were adequately modeled. Moving the location of the slots forward and using all of the inlet surfaces may increase the efficiency of the slot design and reduce the Mach number of the flow through the slots. However, there may be a maximum usefulness of slots.
2. The slit design results shows that a triangle cut may not be the most efficient at relieving pressure. It can be seen that Case 3 was more effective than Case 1 in allowing the shock to proceed downstream, and the only major difference between the two cases, besides the area used to create each triangle, is the width of the designed opening. Therefore, the crotch location can be calculated the same, but a parabolic or 'U' curve that spans the entire inlet bottom may produce a better relief area than the designed triangles presented.
3. The slit design requires a method which predicts the relief area needed in order to swallow the shock. This method will have to account for jet flow effects. Research similar to that used in estimating the bleed slot areas would assist in the design of the areas for the slits. Also, the slits may have to be placed on multiple surfaces.

4. Upon final conclusion, the slit case appears to hold the most promise in creating a simple starting technique. The slot cases show that the initial pressure increase through the inlet is too great to be swallowed by relief downstream of the original crotch. This is collaborated by the fact that the smaller sized slit in Case 1 performed just as well as the redesigned slots in Case 5 for similar flight condition. Equal performance was observed even though the designed slot area was twice the size of the slit area. Therefore, these results show that a relief at the lip of the inlet has far greater potential in relieving pressure than slots downstream.
5. The basic assumptions of quasi one dimensional flow may be an oversimplification of the problem because of the effects of jet flow. Quasi one dimensional flow assumes that velocities, other than the streamwise velocity, are negligible. Jet flow effects create significant cross stream velocities that must be considered.
6. The isentropic area contraction may not be a good representation of what occurs inside the inlet. While the assumption worked in previous research (17), that research was done on a fully symmetric Busemann inlet, and a relatively simple streamline traced inlet (a sugar scoop). Therefore the complex angles, geometries, resulting shocks, and jet flow areas found in the Mustang II inlet may cause the velocity to slow following a different pattern than the isentropic area contraction ratio.

Suggestions for Further Study

The results of this analysis show that research is still needed in bleed systems for inward turning inlets. More specifically, this investigation has shown that the slit geometries should be studied in more detail, with the possible use of smaller slots as a secondary relief system. Theoretically based methods need to be created in order to properly size the slit area while accounting for the jet flow effects that occurred in the presented results. Such relief may call for design openings to be made on multiple surfaces, not just the bottom surface as was the practice presented in this work. Also, since the areas would have to be larger than those calculated here, a mechanism may be required to close some of the open area in an attempt to recover some of the losses once the inlet has started.

The results of this investigation also show that more understanding is needed in the area of large scale bleed systems. While most of the research studied for this work focused on removing boundary layers, little information was found on characterizing large scale bleed systems where significant amounts of the flow needed to be removed. Trends, similar to those presented by Syberg (17), should be determined for bleed systems, similar to slots and slits, where large quantities of the flow must be diverted in an attempt to quantify the jet flow effects revealed in this analysis. Also, inlet geometry should be studied in an attempt to see if complex three dimensional designs present complexities not seen in simple geometries. These results would assist the design of the new slit methods described above.

Bibliography

1. Aeronautics Systems Center Major Shared Resource Center, http://www.asc.hpc.mil/

2. Anderson, J.D., *Modern Compressible Flow: with Historical Perspective*, 3rd ed, McGraw Hill, New York, New York, 2003.

3. Billig, F. S., and Kothari, A. P., "Streamline Tracing: Techniques for Designing Hypersonic Vehicles," American Institute of Aeronautics and Astronautics, Inc., AIAA-ISABE XIII International Symposium on Air Breathing Engines, Chattanooga, TN, 8-12 Sep 1997.

4. CFD++ User Manual – Version 2.6.5

5. Eurofighter Typhoon, http://www.eurofighter.starstreak.net/common/AA/bvraam.html

6. Fleeman, E. L., *Tactical Missile Design*, American Institute of Aeronautics and Astronautics, Inc., Reston, VA, 2001.

7. Kantrowitz, A., and Donaldson, C., "Preliminary Investigation of Supersonic Diffusers," NACA ACR No. L5D20, 1945.

8. Luidens, R. W., and Flaherty, R. J., "Use of Shock-trap Bleed to Improve Recovery of Fixed- and Variable-capture-area Internal-contraction Inlets: Mach Number 2.0 to 3.0," NACA RM E58D24, 1958.

9. Mack, J.D., Private communications/Meeting Notes with Glenn Liston, Mark Hagenmaier, and Lance Jacobsen, Oct 2004 – May 2005.

10. Mattingly, J. D., Heiser, W. H., and Pratt, D. T, *Aircraft Engine Design*, 2nd ed, American Institute of Aeronautics and Astronautics, Inc., Reston, VA, 2002.

11. Molder, S., and Szpiro, E. J., "Busemann Inlet for Hypersonic Speeds," *Journal of Spacecraft and Rockets*, Vol. 3, pp. 1303-1304, Aug 1966.

12. Pointwise: Gridgen Basic Information, http://www.pointwise.com/gridgen/

13. Rhinoceros: NURBS Modeling for Windows Basic Information, http://www.rhino3d.com/

14. Schlichting, H., and Gersten, K., *Boundary Layer Theory*, 8th ed, Springer-Verlag Berlin Heidelberg, Germany, 2000.

15. Sharp, B. M., and Howe, J. P., *Procedures for Estimating Inlet External and Internal Performance*, NWC TP 5555, Naval Weapons Center, China Lake, CA, 1974.

16. Smart, M. K., and Trexler, C. A., "Mach 4 Performance of Hypersonic Inlet with Rectangular-to-Elliptical Shape Transition," *Journal of Propulsion and Power*, Vol. 20, No. 2, March-April 2004.

17. Syberg, J., and Hickcox, T. E., "Design of a Bleed System for a Mach 3.5 Inlet," NASA CR – 2187, 1973.

18. Tam, C., Baurle, R. A., Streby, G. D. "Numerical Analysis of Streamline-Traced Hypersonic Inlets," AAIA 2003-0013, American Institute of Aeronautics and Astronautics, Inc., 41st Aerospace Sciences Meeting and Exhibit, Reno, Nevada, Jan 6-9, 2003.

19. United Stated Navy Fact File, AIM -120 AMRAAM, http://www.chinfo.navy.mil/navpalib/factfile/missiles/wep-amr.html

20. Valorani, M., Nasuti, F., Onofri, M., Buongiorno, C., "Optimal Supersonic Intake Design for Air Collection Engines (ACE)," *Acta Astronautica*, Vol. 45, No. 12, pp. 729-745, 1999.

21. Van Wie, D. M, Molder, S., "Applications of Busemann Inlet Designs for Flight at Hypersonic Speeds," American Institute of Aeronautics and Astronautics, Inc., Aerospace Design Conference, Irvine, CA, Feb 3-6,1992.

Vita

A recent graduate from the University of Notre Dame, Ensign John Mack was designated as a pilot candidate and chose to pursue a Masters degree under the Navy Immediate Graduate Education Program (IGEP). After acceptance into the program, the Air Force Institute of Technology was designated as his first duty assignment where he would earn a Master's degree in Aeronautical engineering. Upon completion of the IGEP program, he will report to NAS Pensacola in order to begin initial flight training. Ensign Mack is currently engaged and will be wed before reporting to NAS Pensacola.

REPORT DOCUMENTATION PAGE

Form Approved
OMB No. 074-0188

1. REPORT DATE *(DD-MM-YYYY)*	**2. REPORT TYPE**	**3. DATES COVERED** *(From – To)*
13-06-2005	Master's Thesis	June 2004 – June 2005

4. TITLE AND SUBTITLE

An Investigation of Starting Techniques for Inward Turning Inlets at Flight Speeds Below the On-Design Mach Number

5a. CONTRACT NUMBER

5b. GRANT NUMBER

5c. PROGRAM ELEMENT NUMBER

6. AUTHOR(S)

John D. Mack, Ensign, USNR

5d. PROJECT NUMBER

5e. TASK NUMBER

5f. WORK UNIT NUMBER

7. PERFORMING ORGANIZATION NAMES(S) AND ADDRESS(S)
Air Force Institute of Technology
Graduate School of Engineering and Management (AFIT/EN)
2950 Hobson Way
WPAFB OH 45433-8865

8. PERFORMING ORGANIZATION REPORT NUMBER

AFIT/GAE/ENY/05-J07

9. SPONSORING/MONITORING AGENCY NAME(S) AND ADDRESS(ES)
Glenn Liston
Aerospace Propulsion Division
Propulsion Directorate (AFRL/PRAT)
1950 Fifth Street
Wright-Patterson AFB OH 45433-7251

10. SPONSOR/MONITOR'S ACRONYM(S) AFRL/PRAT

11. SPONSOR/MONITOR'S REPORT NUMBER(S)

12. DISTRIBUTION/AVAILABILITY STATEMENT

APPROVED FOR PUBLIC RELEASE; DISTRIBUTION UNLIMITED.

13. SUPPLEMENTARY NOTES

14. ABSTRACT The purpose of this study was to create and investigate starting techniques aimed at allowing complex, three dimensional inward turning inlets to start by swallowing the shock wave associated with un-started inlets. The designed techniques were rooted in supersonic diffuser theory and the Kantrowitz limit, and the techniques attempted to alleviate the over contraction that occurs in inward turning inlets at flight speeds below the on-design Mach number. Five cases, three geometries at two flow conditions, and the base non-modified inlet at the two different flow conditions were generated and all were numerically simulated using a commercially produced numerical solver, CFD++. The simulations were computed using the inviscid Navier-Stokes/Euler equations in a steady state analysis to generate the shock wave, followed by a transient analysis to allow the shock to move in time. The results of the investigation show that all five cases proved to be sub-optimal as none were able to successfully swallow the shock during the transient simulation. However, the results from this analysis indicate that the slit case, designs that extended the initial spill areas of the inlet, appear to hold the most potential in the creation of a successful starting technique. The slit case holds the most potential because the slit Mach 2.7 case was just as effective as the slot Mach 2.7 case, yet the slit area was half the size as the designed slots. Future research should attempt to characterize the effects of slits at different Mach numbers and at various complexities of inlet and slit geometry.

15. SUBJECT TERMS
Busemann Inlet, Inward Turning Inlet, Inlet Starting, Starting Techniques, Supersonic Inlet

16. SECURITY CLASSIFICATION OF:			**17. LIMITATION OF ABSTRACT**	**18. NUMBER OF PAGES**	**19a. NAME OF RESPONSIBLE PERSON**
a. REPORT	**b. ABSTRACT**	**c. THIS PAGE**			Dr. Milton Franke
U	**U**	**U**	**UU**	80	**19b. TELEPHONE NUMBER** *(Include area code)* (937) 785-3636 x4720 (mfranke@afit.edu)